ACKNOWLEDGMENTS

The authors thank Tomoko Obama for technical assistance.

REFERENCES

Abbracchio MP, Burnstock G. 1994. Purinoceptors: are there families of P2X and P2Y purinoceptors? Pharmacol Ther 64:445–475.

Abbracchio MP, Ceruti S, Barbieri D, Franceschi C, Malorni W, Biondo L, Burnstock G, Cattabeni F. 1995. A novel action for adenosine: apoptosis of astroglial cells in rat brain primary cultures. Biochem Biophys Res Commun 213:908–915.

Agardh CD, Zhang H, Smith ML, Siesjo BK. 1991. Free radical production and ischemic brain damage: influence of postischemic oxygen tension. Int J Dev Neurosci 9:127–138.

Ahmed SM, Rzigalinski BA, Willoughby KA, Sitterding HA, Ellis EF. 2000. Stretch-induced injury alters mitochondrial membrane potential and cellular ATP in cultured astrocytes and neurons. J Neurochem 74:1951–1960.

Aihara H, Fujiwara S, Mizuta I, Tada H, Kanno T, Tozaki H, Nagai K, Yajima Y, Inoue K, Kondoh T, Motooka Y, Nishizaki T. 2002. Adenosine triphosphate accelerates recovery from hypoxic/hypoglycemic perturbation of guinea pig hippocampal neurotransmission via a P_2 receptor. Brain Res 952:31–37.

Akbar GK, Dasari VR, Webb TE, Ayyanathan K, Pillarisetti K, Sandhu AK, Athwal RS, Daniel JL, Ashby B, Barnard EA, Kunapulis SP. 1996. Molecular cloning of a novel P2 purinoceptor from human erythroleukemia cells. J Biol Chem 271:18363–18367.

Altman FP. 1976. Tetrazolium salts: a consumer's guide. Histochem J 8:471–485.

Appel E, Kazimirsky G, Ashkenazi E, Kim SG, Jacobson KA, Brodie C. 2001. Roles of BCL-2 and caspase 3 in the adenosine A3 receptor-induced apoptosis. J Mol Neurosci 17:285–292.

Araque A, Parpura V, Sanzgiri RP, Haydon PG. 1999a. Tripartite synapses: glia, the unacknowledged partner. Trends Neurosci 22: 208–215.

Araque A, Sanzgiri RP, Parpura V, Haydon PG. 1999b. Astrocyte-induced modulation of synaptic transmission. Can J Physiol Pharmacol 77:699–706.

Araque A, Carmignoto G, Haydon PG. 2001. Dynamic signaling between astrocytes and neurons. Annu Rev Physiol 63:795–813.

Ayyanathan K, Webbs TE, Sandhu AK, Athwal RS, Barnard EA, Kunapuli SP. 1996. Cloning and chromosomal localization of the human $P2Y_1$ purinoceptor. Biochem Biophys Res Commun 218: 783–788.

Balcz B, Kirchner L, Cairns N, Fountoulakis M, Lubec G. 2001. Increased brain protein levels of carbonyl reductase and alcohol dehydrogenase in Down syndrome and Alzheimer's disease. J Neural Transm Suppl;(61):193–201.

Behan WM, Stone TW. 2002. Enhanced neuronal damage by co-administration of quinolinic acid and free radicals, and protection by adenosine A2A receptor antagonists. Br J Pharmacol 135:1435–1442.

Brambilla R, Burnstock G, Bonazzi A, Ceruti S, Cattabeni F, Abbracchio MP. 1999. Cyclo-oxygenase-2 mediates P2Y receptor-induced reactive astrogliosis. Br J Pharmacol 126:563–567.

Braun N, Lenz C, Gillardon F, Zimmermann M, Zimmermann H. 1997. Focal cerebral ischemia enhances glial expression of ecto-5'-nucleotidase. Brain Res 766:213–226.

Braun N, Zhu Y, Krieglstein J, Culmsee C, Zimmermann H. 1998. Upregulation of the enzyme chain hydrolyzing extracellular ATP after transient forebrain ischemia in the rat. J Neurosci 18:4891–4900.

Butterfield DA, Boyd-Kimball D, Castegna A. 2003. Proteomics in Alzheimer's disease: insights into potential mechanisms of neurodegeneration. J Neurochem 86:1313–1327.

Ceruti S, Franceschi C, Barbieri D, Malorni W, Camurri A, Giammarioli AM, Ambrosini A, Racagni G, Cattabeni F, Abbracchio MP. 2000. Apoptosis induced by 2-chloro-adenosine and 2-chloro-2'-deoxy-adenosine in a human astrocytoma cell line: differential mechanisms and possible clinical relevance. J Neurosci Res 60:388–400.

Charles AC, Merrill JE, Dirksen ER, Sanderson MJ. 1991. Intercellular signaling in glial cells: calcium waves and oscillations in response to mechanical stimulation and glutamate. Neuron 6:983–992.

Chen J, Backus KH, Deitmer JW. 1997. Intracellular calcium transients and potassium current oscillations evoked by glutamate in cultured rat astrocytes. J Neurosci 17:7278–7287.

Ciccarelli R, Ballerini P, Sabatino G, Rathbone MP, D'Onofrio M, Caciagli F, Di Iorio P. 2001. Involvement of astrocytes in purine-mediated reparative processes in the brain. Int J Dev Neurosci 19:395–414.

Cornell-Bell AH, Finkbeiner SM, Cooper MS, Smith SJ. 1990. Glutamate induces calcium waves in cultured astrocytes: long-range glial signaling. Science 247:470–473.

Cuajungco MP, Goldstein LE, Nunomura A, Smith MA, Lim JT, Atwood CS, Huang X, Farrag YW, Perry G, Bush AI. 2000. Evidence that the beta-amyloid plaques of Alzheimer's disease represent the redox-silencing and entombment of abeta by zinc. J Biol Chem 275:19439–19442.

Desagher S, Glowinski J, Premont J. 1996. Astrocytes protect neurons from hydrogen peroxide toxicity. J Neurosci 16:2553–2562.

Di Iorio P, Kleywegt S, Ciccarelli R, Traversa U, Andrew CM, Crocker CE, Werstiuk ES, Rathbone MP. 2002. Mechanisms of apoptosis induced by purine nucleosides in astrocytes. Glia 38:179–190.

Dubyak GR, el-Moatassim C. 1993. Signal transduction via P2-purinergic receptors for extracellular ATP and other nucleotides. Am J Physiol 265(3 Pt 1):C577–606.

Eftekharpour E, Holmgren A, Juurlink BH. 2000. Thioredoxin reductase and glutathione synthesis is upregulated by t-butylhydroquinone in cortical astrocytes but not in cortical neurons. Glia 31:241–248.

Fam SR, Gallagher CJ, Salter MW. 2000. $P2Y_1$ purinoceptor-mediated Ca^{2+} signaling and Ca^{2+} wave propagation in dorsal spinal cord astrocytes. J Neurosci 20:2800–2808.

Finkbeiner S. 1992. Calcium waves in astrocytes-filling in the gaps. Neuron 8:1101–1108.

Forrest GL, Gonzalez B. 2000. Carbonyl reductase. Chem Biol Interact 129:21–40.

Franke H, Grosche J, Schadlich H, Krugel U, Allgaier C, Illes P. 2001a. P2X receptor expression on astrocytes in the nucleus accumbens of rats. Neuroscience 108:421–429.

Franke H, Krugel U, Schmidt R, Grosche J, Reichenbach A, Illes P. 2001b. P2 receptor-types involved in astrogliosis in vivo. Br J Pharmacol 134:1180–1189.

Fredholm BB, Dunwiddie TV. 1988. How does adenosine inhibit transmitter release? Trends Pharmacol Sci 9:130–134.

Fumagalli M, Brambilla R, D'Ambrosi N, Volonte C, Matteoli M, Verderio C, Abbracchio MP. 2003. Nucleotide-mediated calcium signaling in rat cortical astrocytes: role of P2X and P2Y receptors. Glia 43:218–230.

Furuta A, Price DL, Pardo CA, Troncoso JC, Xu ZS, Taniguchi N, Martin LJ. 1995. Localization of superoxide dismutases in Alzheimer's disease and Down's syndrome neocortex and hippocampus. Am J Pathol 146:357–367.

Gallagher CJ, Salter MW. 2003. Differential properties of astrocyte calcium waves mediated by $P2Y_1$ and $P2Y_2$ receptors. J Neurosci 23:6728–6739.

Glaum SR, Holzwarth JA, Miller RJ. 1990. Glutamate receptors activate Ca^{2+} mobilization and Ca^{2+} influx into astrocytes. Proc Natl Acad Sci USA 87:3454–3458.

Guthrie PB, Knappenberger J, Segal M, Bennett MV, Charles AC, Kater SB. 1999. ATP released from astrocytes mediates glial calcium waves. J Neurosci 19:520–528.

Hansson HA, Holmgren A, Norstedt G, Rozell B. 1989. Changes in the distribution of insulin-like growth factor I, thioredoxin, thioredoxin reductase and ribonucleotide reductase during the development of the retina. Exp Eye Res 48:411–420.

Haydon PG. 2001. Glia: listening and talking to the synapse. Nat Rev Neurosci 2:185–193.

Hentschel S, Lewerenz A, Nieber K. 2003. Activation of A_3 receptors by endogenous adenosine inhibits synaptic transmission during hypoxia in rat cortical neurons. Restor Neurol Neurosci 21:55–63.

Ho C, Hicks J, Salter MW. 1995. A novel P2-purinoceptor expressed by a subpopulation of astrocytes from the dorsal spinal cord of the rat. Br J Pharmacol 116:2909–2918.

Huang X, Cuajungco MP, Atwood CS, Moir RD, Tanzi RE, Bush AI. 2000. Alzheimer's disease, beta-amyloid protein and zinc. J Nutr 130(5 suppl):1488S-1492S.

Idestrup CP, Salter MW. 1998. P2Y and P2U receptors differentially release intracellular Ca^{2+} via the phospholipase c/inositol 1,4,5-triphosphate pathway in astrocytes from the dorsal spinal cord. Neuroscience 86:913–923.

Inazu N, Ruepp B, Wirth H, Wermuth B. 1992. Carbonyl reductase from human testis: purification and comparison with carbonyl reductase from human brain and rat testis. Biochim Biophys Acta 1116:50–56.

Innocenti B, Parpura V, Haydon PG. 2000. Imaging extracellular waves of glutamate during calcium signaling in cultured astrocytes. J Neurosci 20:1800–1808.
Inoue K, Koizumi S, Nakazawa K. 1995. Glutamate-evoked release of adenosine 5'-triphosphate causing an increase in intracellular calcium in hippocampal neurons. NeuroReport 6:437–440.
James G, Butt AM. 2002. P2Y and P2X purinoceptor mediated $Ca(^{2+})$ signalling in glial cell pathology in the central nervous system. Eur J Pharmacol 447:247–260.
Jones PA, Smith RA, Stone TW. 1998. Protection against hippocampal kainate excitotoxicity by intracerebral administration of an adenosine A2A receptor antagonist. Brain Res 800:328–335.
Jurkowitz MS, Litsky ML, Browning MJ, Hohl CM. 1998. Adenosine, inosine, and guanosine protect glial cells during glucose deprivation and mitochondrial inhibition: correlation between protection and ATP preservation. J Neurochem 71:535–548.
Kim SG, Gao ZG, Soltysiak KA, Chang TS, Brodie C, Jacobson KA. 2003a. P2Y6 nucleotide receptor activates PKC to protect 1321N1 astrocytoma cells against tumor necrosis factor-induced apoptosis. Cell Mol Neurobiol 23:401–418.
Kim SG, Soltysiak KA, Gao ZG, Chang TS, Chung E, Jacobson KA. 2003b. Tumor necrosis factor alpha-induced apoptosis in astrocytes is prevented by the activation of P2Y6, but not $P2Y_4$ nucleotide receptors. Biochem Pharmacol 65:923–931.
Kim SH, Vlkolinsky R, Cairns N, Fountoulakis M, Lubec G. 2001. The reduction of NADH ubiquinone oxidoreductase 24- and 75-kDa subunits in brains of patients with Down syndrome and Alzheimer's disease. Life Sci 68:2741–2750.
Koizumi S, Inoue K. 1997. Inhibition by ATP of calcium oscillations in rat cultured hippocampal neurones. Br J Pharmacol 122:51–58.
Koizumi S, Saito Y, Nakazawa K, Nakajima K, Sawada JI, Kohsaka S, Illes P, Inoue K. 2002. Spatial and temporal aspects of Ca^{2+} signaling mediated by P2Y receptors in cultured rat hippocampal astrocytes. Life Sci 72:431–442.
Koizumi S, Fujishita K, Tsuda M, Shigemoto-Mogami Y, Inoue K. 2003. Dynamic inhibition of excitatory synaptic transmission by astrocyte-derived ATP in hippocampal cultures. Proc Natl Acad Sci USA 100:11023–11028.
Lei B, Adachi N, Arai T. 1997. The effect of hypothermia on H_2O_2 production during ischemia and reperfusion: a microdialysis study in the gerbil hippocampus. Neurosci Lett 222:91–94.
Lenz G, Gottfried C, Luo Z, Avruch J, Rodnight R, Nie WJ, Kang Y, Neary JT. 2000. P_{2Y} purinoceptor subtypes recruit different mek activators in astrocytes. Br J Pharmacol 129:927–936.
Lovell MA, Xie C, Gabbita SP, Markesbery WR. 2000. Decreased thioredoxin and increased thioredoxin reductase levels in Alzheimer's disease brain. Free Radic Biol Med 28:418–427.
Lustig KD, Shiau AK, Brake AJ, Julius D. 1993. Expression cloning of an ATP receptor from mouse neuroblastoma cells. Proc Natl Acad Sci USA 90:5113–5117.
Lutz PL, Kabler S. 1997. Release of adenosine and ATP in the brain of the freshwater turtle (*Trachemys scripta*) during long-term anoxia. Brain Res 769:281–286.
Moore D, Iritani S, Chambers J, Emson P. 2000. Immunohistochemical localization of the $P2Y_1$ purinergic receptor in Alzheimer's disease. NeuroReport 11:3799–3803.
Neary JT, Kang Y, Bu Y, Yu E, Akong K, Peters CM. 1999. Mitogenic signaling by ATP/P2Y purinergic receptors in astrocytes: involvement of a calcium-independent protein kinase C, extracellular signal-regulated protein kinase pathway distinct from the phosphatidylinositol-specific phospholipase C/calcium pathway. J Neurosci 19:4211–4220.
Newman EA. 2003. Glial cell inhibition of neurons by release of ATP. J Neurosci 23:1659–1666.
Panenka W, Jijon H, Herx LM, Armstrong JN, Feighan D, Wei T, Yong VW, Ransohoff RM, MacVicar BA. 2001. P2X7-like receptor activation in astrocytes increases chemokine monocyte chemoattractant protein-1 expression via mitogen-activated protein kinase. J Neurosci 21:7135–7142.
Parkinson FE, Sinclair CJ, Othman T, Haughey NJ, Geiger JD. 2002. Differences between rat primary cortical neurons and astrocytes in purine release evoked by ischemic conditions. Neuropharmacology 43:836–846.
Parpura V, Basarsky TA, Liu F, Jeftinija K, Jeftinija S, Haydon PG. 1994. Glutamate-mediated astrocyte-neuron signalling. Nature 369:744–747.
Pasti L, Volterra A, Pozzan T, Carmignoto G. 1997. Intracellular calcium oscillations in astrocytes: a highly plastic, bidirectional form of communication between neurons and astrocytes in situ. J Neurosci 17:7817–7830.
Peakman MC, Hill SJ. 1994. Adenosine A2B-receptor-mediated cyclic AMP accumulation in primary rat astrocytes. Br J Pharmacol 111: 191–198.
Porter JT, McCarthy KD. 1995. Adenosine receptors modulate $[Ca^{2+}]_i$ in hippocampal astrocytes in situ. J Neurochem 65:1515–1523.
Porter JT, McCarthy KD. 1996. Hippocampal astrocytes in situ respond to glutamate released from synaptic terminals. J Neurosci 16:5073–5081.
Queiroz G, Meyer DK, Meyer A, Starke K, von Kugelgen I. 1999. A study of the mechanism of the release of ATP from rat cortical astroglial cells evoked by activation of glutamate receptors. Neuroscience 91:1171–1181.
Rozell B, Hansson HA, Luthman M, Holmgren A. 1985. Immunohistochemical localization of thioredoxin and thioredoxin reductase in adult rats. Eur J Cell Biol 38:79–86.
Schipke CG, Boucsein C, Ohlemeyer C, Kirchhoff F, Kettenmann H. 2002. Astrocyte Ca^{2+} waves trigger responses in microglial cells in brain slices. FASEB J 16:255–257.
Schubert P, Ogata T, Marchini C, Ferroni S, Rudolphi K. 1997. Protective mechanisms of adenosine in neurons and glial cells. Ann NY Acad Sci 825:1–10.
Schwarzschild MA, Xu K, Oztas E, Petzer JP, Castagnoli K, Castagnoli N Jr, Chen JF. 2003. Neuroprotection by caffeine and more specific A2A receptor antagonists in animal models of Parkinson's disease. Neurology 61(11 suppl 6):S55–61.
Servitja JM, Masgrau R, Pardo R, Sarri E, Picatoste F. 2000. Effects of oxidative stress on phospholipid signaling in rat cultured astrocytes and brain slices. J Neurochem 75:788–794.
Shahidullah M, Wilson WS. 1997. Mobilisation of intracellular calcium by $P2Y_2$ receptors in cultured, non-transformed bovine ciliary epithelial cells. Curr Eye Res 16:1006–1016.
Shin CY, Choi JW, Ryu JR, Ko KH, Choi JJ, Kim HS, Lee JC, Lee SJ, Kim HC, Kim WK. 2002. Glucose deprivation decreases nitric oxide production via NADPH depletion in immunostimulated rat primary astrocytes. Glia 37:268–274.
Tabner BJ, Turnbull S, El-Agnaf O, Allsop D. 2001. Production of reactive oxygen species from aggregating proteins implicated in Alzheimer's disease, Parkinson's disease and other neurodegenerative diseases. Curr Top Med Chem 1:507–517.
Tamagno E, Robino G, Obbili A, Bardini P, Aragno M, Parola M, Danni O. 2003. H_2O_2 and 4-hydroxynonenal mediate amyloid beta-induced neuronal apoptosis by activating JNKs and p38MAPK. Exp Neurol 180:144–155.
Tokuyama Y, Hara M, Jones EM, Fan Z, Bell GI. 1995. Cloning of rat and mouse P2Y purinoceptors. Biochem Biophys Res Commun 211: 211–218.
Twentyman PR, Luscombe M. 1987. A study of some variables in a tetrazolium dye (MTT) based assay for cell growth and chemosensitivity. Br J Cancer 56:279–285.
Verderio C, Matteoli M. 2001. ATP mediates calcium signaling between astrocytes and microglial cells: modulation by IFN-gamma. J Immunol 166:6383–6391.
Viana F, de Smedt H, Droogmans G, Nilius B. 1998. Calcium signalling through nucleotide receptor $P2Y_2$ in cultured human vascular endothelium. Cell Calcium 24:117–127.
Webb TE, Simon J, Barnard EA. 1998. Regional distribution of [35S]2'-deoxy 5'-O-(1-thio) ATP binding sites and the $P2Y_1$ messenger RNA within the chick brain. Neuroscience 84:825–837.
Wieraszko A, Goldsmith G, Seyfried TN. 1989. Stimulation-dependent release of adenosine triphosphate from hippocampal slices. Brain Res 485:244–250.
Wirth H, Wermuth B. 1992. Immunohistochemical localization of carbonyl reductase in human tissues. J Histochem Cytochem 40: 1857–1863.
Yamakuni H, Kawaguchi N, Ohtani Y, Nakamura J, Katayama T, Nakagawa T, Minami M, Satoh M. 2002. ATP induces leukemia inhibitory factor mRNA in cultured rat astrocytes. J Neuroimmunol 129:43–50.
Zhang JM, Wang HK, Ye CQ, Ge W, Chen Y, Jiang ZL, Wu CP, Poo MM, Duan S. 2003. ATP released by astrocytes mediates glutamatergic activity-dependent heterosynaptic suppression. Neuron 40: 971–982.
Zhang M, Zhong H, Vollmer C, Nurse CA. 2000. Co-release of ATP and ACh mediates hypoxic signalling at rat carotid body chemoreceptors. J Physiol 525(Pt 1):143–158.
Zimmermann H. 1996. Biochemistry, localization and functional roles of ecto-nucleotidases in the nervous system. Prog Neurobiol 49: 589–618.

Available online at www.sciencedirect.com
SCIENCE DIRECT
ELSEVIER
Biochemical Pharmacology 68 (2004) 2177–2186
Biochemical Pharmacology
www.elsevier.com/locate/biochempharm

Differential modulation of PI3-kinase/Akt pathway during all-*trans* retinoic acid- and Am80-induced HL-60 cell differentiation revealed by DNA microarray analysis

Seiichi Ishida[a,*], Yukari Shigemoto-Mogami[b], Youichi Shinozaki[b], Hiroyuki Kagechika[c,1], Koichi Shudo[d], Shogo Ozawa[a], Jun-ichi Sawada[e], Yasuo Ohno[a], Kazuhide Inoue[b]

[a]*Division of Pharmacology, National Institute of Health Sciences, 1-18-1 Kamiyoga, Setagaya-ku, Tokyo 158-8501, Japan*
[b]*Division of Biosignaling, National Institute of Health Sciences, 1-18-1 Kamiyoga, Setagaya-ku, Tokyo 158-8501, Japan*
[c]*Graduate School of Pharmaceutical Sciences, The University of Tokyo, 7-3-1 Hongo, Bunkyo-ku, Tokyo 113-0033, Japan*
[d]*ITSUU Laboratory, 2-28-10 Tamagawa, Setagaya-ku, Tokyo 158-0094, Japan*
[e]*Division of Biochemistry and Immunochemistry, National Institute of Health Sciences, 1-18-1 Kamiyoga, Setagaya-ku, Tokyo 158-8501, Japan*

Received 21 April 2004; accepted 4 August 2004

Abstract

All-*trans* retinoic acid (ATRA) and Am80 are natural and synthetic derivatives of Vitamin A and have been used in the fields of oncology and dermatology for years. Their action was considered to be achieved mainly through binding to nuclear hormone receptors, retinoic acid receptors (RARs), although they have been observed to have different biological effects. For example, the two compounds have similar effects on differentiation but different effects on proliferation in human promyelocytic leukemia cell line HL-60 cells. To elucidate the genes responsible for this and other differences, we attempted for the first time to determine the genes whose expressions were differentially modulated during the time course of HL-60 cell differentiation by ATRA and Am80 treatment up to 72 h utilizing DNA microarray and clustering analyses. As a result, the expressions of 204 genes were found to be modulated differentially by ATRA and Am80. Among them, we focused on two components of the PI3-kinase/Akt signal transduction pathway, *phosphoinositide-3-kinase, β-catalytic subunit* and *ribosomal protein S6 kinase polypeptide 1*, which are related to the regulation of cell proliferation and apoptosis. Their expressions were specifically suppressed by ATRA, which coincided with the suppressive effects of ATRA on the HL-60 cell proliferation. Moreover, PI3-kinase inhibitors suppressed the proliferation of Am80-treated cells to the same extent as ATRA did. These results indicated that these gene products play a role in HL-60 cell growth suppression during the late stage of differentiation. The complete data and a list of the genes are available at http://www.nihs.go.jp/mpj/index-e.htm.

Keywords: All-*trans* retinoic acid; Am80; HL-60; Cell proliferation; Global gene expression profiling analysis; PI3-kinase/Akt pathway

1. Introduction

Retinoids are natural or synthetic derivatives of Vitamin A and have potential chemopreventive and therapeutic applications in the fields of oncology and dermatology. One of the successful applications of retinoids is for differentiation therapy in acute promyelocytic leukemia (APL) using all-*trans* retinoic acid (ATRA) (Fig. 1). In most cases, high complete remission rates were achieved in APL with ATRA treatment, a result much better than that provided by conventional chemotherapy [1]. Now, ATRA is the first-choice drug in APL treatment. As the therapeutic applications of retinoids have become wider, a number of synthetic retinoids have been developed. Among them, Am80 (Fig. 1) has been used already in the treatment of APL in a clinical trial and showed better potency [2,3]. Am80 was able to introduce a second complete remission in 58% of the patients who relapsed after the first ATRA treatment and with fewer adverse effects. Am80, as well as many other synthetic retinoids, has been developed by an in vitro differentiation assay

Abbreviations: APL, acute promyelocytic leukemia; ATRA, all-*trans* retinoic acid; 9-*cis* RA, 9-*cis* retinoic acid

* Corresponding author. Tel.: +81 3 5717 3831; fax: +81 3 5717 3832.
E-mail address: ishida@nihs.go.jp (S. Ishida).
[1] Present address: School of Biomedical Sciences, Tokyo Medical and Dental University, 2-3-10 Kanda-Surugadai, Chiyoda-ku, Tokyo 101-0062, Japan.

0006-2952/$ – see front matter © 2004 Elsevier Inc. All rights reserved.
doi:10.1016/j.bcp.2004.08.017

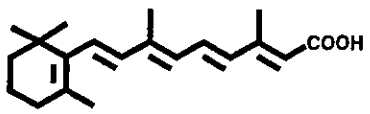

ATRA

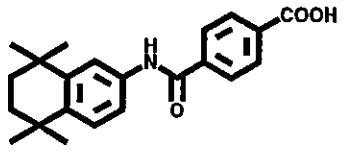

Am80

Fig. 1. Structures of retinoids used in this study.

using HL-60 human promyelocytic leukemia cell line [4] and it was approximately 10 times more potent than ATRA in differentiation induction activity. This and other unique features of Am80 were suggested to explain its higher potency in APL treatments [2,3]. In addition to these features of Am80, Am80 showed different effects on HL-60 cell growth during the differentiation assay compared to ATRA. The cells treated with Am80 for 4 days (the normal period of the assay) were growing with the slower growth rate, while ATRA-treated cells almost ceased growing [5][1], indicating that ATRA suppressed the cell growth much more strongly than Am80.

Both ATRA and Am80 are thought to exert their biological effects through binding to retinoic acid receptors (RARs), members of the nuclear steroid hormone receptors. Biochemical analysis of their binding proteins in HL-60 cell extracts clearly showed that the major binding proteins were RARs [6,7]. This suggested that they should have common biological activities. However, ATRA showed binding to several other proteins in the same assay. This implies that ATRA and Am80 should have different biological or clinical activities, such as the differences in the effects of growth suppression observed in HL-60 cell cultures or the side-effects experienced in clinical applications which are usually severer in ATRA treatment. These facts prompted us to clarify the differences and the similarities of ATRA and Am80, because it should provide important information for the development of retinoids with more potency and/or fewer side-effects. For this purpose, we conducted a large-scale analysis of the gene expression using DNA microarray and clustering analysis to elucidate the genes whose expressions were differentially modulated during the time course of HL-60 cell differentiation by ATRA and Am80.

2. Materials and methods

2.1. Chemicals

ATRA and LY294002 were purchased from Sigma Chemical Co. Wortmannin was purchased from Wako Pure Chemicals. Am80 [8] and PA024 [9] were synthesized at The University of Tokyo. All chemicals were dissolved in ethanol.

2.2. Cells, cell culture, and cell treatments

The human promyelocytic leukemia cells, HL-60, were provided by Dr. F. Takaku (Faculty of Medicine, The University of Tokyo). The cells were cultured in suspension in RPMI-1640 (Biomedicals Inc.) supplemented with 5% fetal bovine serum (BioWhittaker or Wako Pure Chemicals) and penicillin–streptomycin (Invitrogen) under a humidified atmosphere of 5% CO_2 at 37 °C. Fetal bovine serum from either provider gave identical results in terms of HL-60 cell differentiation. The following numbers of cells were seeded at the beginning of culture according to the culture period, i.e. 1×10^6 cells/ml for 1 and 9 h culture, 8×10^5 cells/ml for 24 h culture, 3×10^5 cells/ml for 72 h culture, and 1×10^5 cells/ml for 96 h culture. ATRA, Am80, wortmannin, or LY294002 was added to the cells at the indicated time of the culture, and the cells were harvested and processed further at the end of the indicated culture period. The same volume of ethanol was added to the control culture (0.5% (v/v)), which did not affect the HL-60 cell growth and differentiation.

2.3. Total RNA preparation

After washing the cells twice with PBS, total RNA was prepared with RNeasy Mini total RNA Preparation Kit (Qiagen) according to the manufacturer's instructions.

2.4. DNA microarray analysis

Converting total RNA to the targets for Affymetrix GeneChip DNA microarray hybridization was done according to the manufacturer's instructions. The targets were hybridized to a human genome U95A GeneChip DNA microarray (Affymetrix) for 16–24 h at 45 °C. After the hybridization, the DNA microarrays were washed and stained on Fluidics Station (Affymetrix) according to the protocol provided by Affymetrix. Then, the DNA microarrays were scanned, and the images obtained were analyzed by Microarray Suite Expression Analysis Software (version 5.0; Affymetrix). The DNA microarray analysis of each sample was done in duplicate. The results of the DNA microarray analyses are available at our web site, http://www.nihs.go.jp/mpj/index-e.htm.

2.5. Cluster analysis of gene expression patterns induced by ATRA and Am80

The first step was selecting genes whose expressions were changed by either ATRA or Am80 with statistical significance at least at one time point and whose expressions were reproducible through the time course. The data

[1] Ishida et al. unpublished results.

acquired through the absolute analysis by Microarray Suite Expression Analysis Software were imported to the GENFO program [10] due to the limited replicates of the DNA microarray data. GENFO is a suitable program in this case because it selects the genes whose expressions changed by a given treatment with statistical significance based upon the "a priori S.D." "A priori S.D." was obtained from independent experiment beforehand, in which the variation of given signal intensity was determined from six replicate measurements of human genome U95A DNA microarrays [10]. Using this "a priori S.D." avoids the need for many replicates in the actual experiment, which are usually required for conducting *t*-test etc. Genes that showed $p < 0.01$ were selected. Genes whose duplicate measurements by GeneChip differed more than those expected by the a priori S.D. were also eliminated during this step. Then the fold change of each gene by either ATRA or Am80 treatment at each time point was calculated. Genes whose expressions changed more than or equal to 2.5-fold were selected. In addition to this, the average expression level ("Signal" value of the Microarray Suite Expression Analysis Software) of a given gene through all the time points of three samples, control, ATRA, and Am80, was calculated and genes which had an average more than or equal to 1000 were selected. The genes which passed all three criteria above were assumed to be the genes whose expressions were changed by either ATRA or Am80 with statistical significance at least at one time point and whose expressions were reproducible through the time course. The number of genes left by this selection was 610. Next, the relative expression level (expression level of ATRA- or Am80-treated sample/expression level of the control sample, the average of duplicate measurements) of each gene during the time course was plotted and successively subjected to hierarchical clustering and *k*-mean clustering (GeneSpring, Silicon Genetics).

3. Results

3.1. Delineation of distinct patterns of gene expressions induced by ATRA and Am80

To elucidate the different effects of ATRA and Am80 on the gene expressions, the expression levels of 12,559 genes in HL-60 cells treated with 0.1 μM ATRA or Am80 for 1, 9, 24, and 72 h were analyzed by Affymetrix human genome U95A GeneChip and genes whose expressions were reproducible and changed more than 2.5-fold by either ATRA or Am80 treatment were selected according to the procedure described in Section 2. Next, to select the genes differentially modulated by ATRA and Am80, the relative expression level (expression level of ATRA- or Am80-treated sample/expression level of control sample) of each gene during the time course was plotted and successively subjected to the hierarchical clustering and *k*-mean clustering. Fifty seven patterns (set 1–set 57) were obtained and are shown in Fig. 2A. The number, 57, was obtained as the result of serial trials to identify the tight clustering by comparing the "percent explained variability" calculated by GeneSpring. To select the patterns which showed different gene expressions by ATRA and Am80, the average relative expression levels of the genes included in each set were calculated, then the similarity of the calculated average relative gene expression levels of ATRA and Am80 were compared by evaluating the standard correlation between them. The sets that showed a standard correlation of less than 0.965, which was set arbitrarily, were judged as "differentially controlled" sets. These sets are highlighted in Fig. 2A and the number of genes involved in these sets was 204. The genes involved in the sets whose standard correlations were greater than or equal to 0.965 (406 genes) were modulated in their expression almost identically by ATRA and Am80. These genes were interesting from a different point of view in so far as they were regulated by both retinoids through RARs in a similar manner, and are thus considered candidate retinoid target genes. The complete list of 610 genes available at our website includes a comparison with the list of retinoic acid target genes reviewed by Balmer and Blomhoff [11]. The fact that two-thirds of the genes clustered showed identical expression patterns by ATRA and Am80 treatment also indicated that the reproducibility of the time course analysis conducted in this study was fairly high (see discussion).

The expression patterns of some of the "differentially controlled" sets appeared visually similar to each other. Thus, to group these sets, hierarchical clustering was applied which compared the similarity of each set by calculating the Pearson correlation coefficients. The result is shown in Fig. 2B. Each node contained the sets whose expression patterns were similar to each other. As a result, there were several groups of genes whose expressions were differentially modulated by ATRA and Am80. The results showed that about one-third of the genes (204 genes out of 610 genes) were controlled differentially by ATRA and Am80, and indicated that ATRA and Am80 actually had different effects upon the gene expressions.

3.2. Identification of genes responsible for the growth suppression by ATRA

One node, which consisted of sets 36, 39, 40, and 47, was interesting for two reasons: The first is that the expressions of the genes involved in this node were suppressed by ATRA but not by Am80. The second is that many of the genes involved in this node were related to cell proliferation and anti-apoptosis (Table 1). Considering that the growth of HL-60 cells was suppressed by ATRA more efficiently than by Am80 during the course of differentiation, the difference in the expression pattern of this node

that contained many cell growth-related genes should explain the different effects of ATRA and Am80 on the cell growth. Thus, we looked closer into the gene list and found two interesting genes, (*phosphoinositide-3-kinase, β-catalytic subunit* and *ribosomal protein S6 kinase polypeptide1*) because they were involved in the same signal transduction pathway, the PI3-kinase/Akt pathway. Keeping this pathway active is important for the cell growth and prevents the cells from undergoing apoptosis [13,18]. The expressions of these two genes were suppressed by ATRA but not by Am80 (see Fig. 4 for the individual expression pattern). Thus, the PI3-kinase/Akt pathway might be suppressed in the ATRA-treated HL-60 cells, while it might be still active in the Am80-treated HL-60 cells. This hypo-

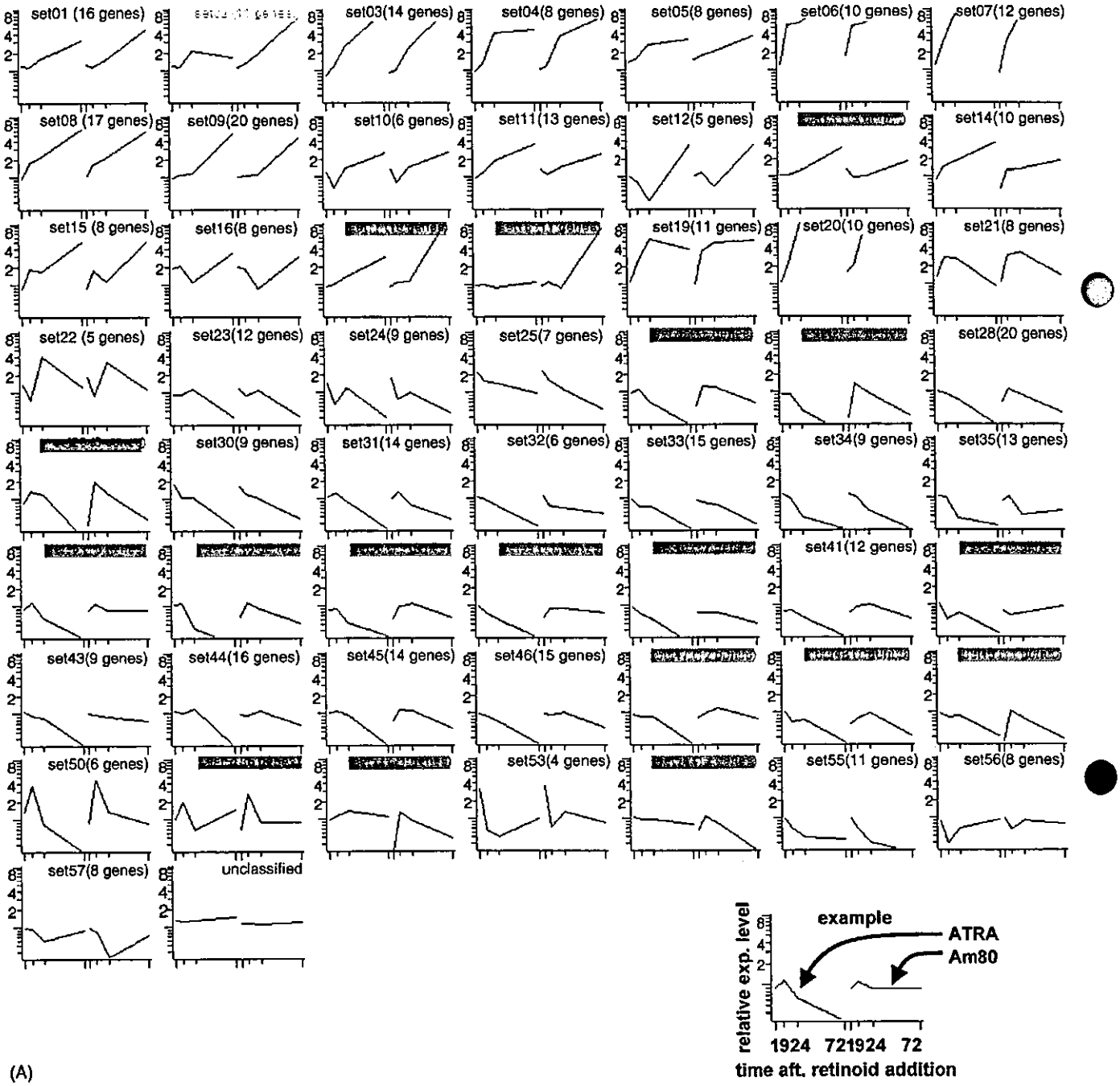

Fig. 2. Selection of gene sets whose expressions were differentially controlled by ATRA and Am80. (A) HL-60 cells were incubated with ATRA, Am80, or ethanol (vehicle) for 1, 9, 24, and 72 h, and the expressions of 12,559 genes on Affymetrix human genome U95A DNA microarray were assayed in duplicate. Genes whose expressions were changed by either ATRA or Am80 with statistical significance were selected and clustered by *k*-mean clustering. Averaged relative expression level of genes included in each set is plotted. Vertical axis is relative expression level and horizontal axis is the time after retinoid addition. Left part of each graph is the expression pattern of the ATRA-treated sample and the right part is that of the Am80-treated one. The sets in which genes were differentially regulated by ATRA and Am80 are highlighted. The set "unclassified" included genes that were eliminated during the selection step. (B) The sets in which genes were differentially regulated by ATRA and Am80 were grouped by hierarchical clustering. Relative expression level of each set is depicted in pseudocolor scale.

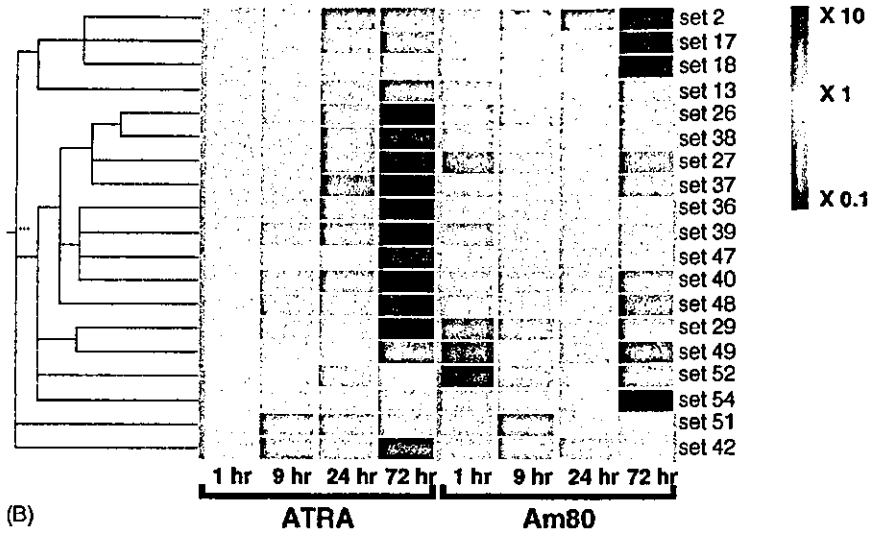

Fig. 2. (*Continued*).

thesis led the idea that if the activity of this pathway were inhibited in the Am80-treated cells, the growth of those cells should be suppressed. We employed two inhibitors, wortmannin and LY294002, for this purpose. HL-60 cells were cultured with or without Am80 (0.1 μM) for 3 days, and then wortmannin (150 nM) or LY294002 (4 μM) was added to the culture medium. To the control culture the same amount of ethanol was added. After 1 day culture with or without inhibitors, the cell number was counted. As shown in Fig. 3A, neither wortmannin nor LY294002 affected the growth of HL-60 cells cultured without Am80. In contrast, when wortmannin or LY294002 was added to the Am80-treated HL-60 cells, both inhibitors suppressed the growth of the cells. The effect of wortmannin was more significant than that of LY294002 since the growth of the cells was suppressed to the same level as ATRA-treated HL-60 cells. The fact that wortmannin is an irreversible inhibitor and LY294002 is a reversible inhibitor might explain this difference. We also checked the dose dependency of the effects of wortmannin and LY294002 in HL-60 cell growth inhibition same as Fig. 3A. The results (Fig. 3B and data not shown) showed that their effects were dose-dependent. These indicated that the suppression of growth at the late stage of differentiation induced by ATRA was caused by the reduced expression of PI3-kinase/Akt pathway component genes, and suppression of this pathway by inhibitors in Am80-treated HL-60 cell mimicked the effect of ATRA on cell growth suppression.

The effects of these inhibitors on HL-60 cell differentiation were also examined using an NBT reduction assay. Am80 alone induced the differentiation of almost 90% of cells at the end of the 4 days of treatment. HL-60 cells treated with Am80 and either inhibitor differentiated almost the same (around 90%; data not shown), indicating that these inhibitors did not affect the HL-60 cell differentiation at this stage.

3.3. Specificity of effects of ATRA on phosphoinositide-3-kinase, β-catalytic subunit and ribosomal protein S6 kinase polypeptide 1 expressions

Both ATRA and Am80 bind RARs selectively. However, ATRA easily transforms to the isomer, 9-*cis* retinoic acid (9-*cis* RA), photochemically. There is a possibility that 9-*cis* RA existing in the culture medium of ATRA-treated cells caused the different effect on HL-60 cell growth, since 9-*cis* RA binds and activates RXR in addition to RAR. To exclude this possibility, RXR ligand PA024 (10 nM) was added with Am80 to the culture medium and the same GeneChip analysis was conducted. PA024 is an RXR-specific ligand [9] and both Am80 and PA024 are stable photochemically or in normal assay conditions. The expression patterns of *phosphoinositide-3-kinase, β-catalytic subunit, ribosomal protein S6 kinase polypeptide 1*, and *c-myc* in ATRA-treated cells, Am80-treated cells, and Am80 with PA024-treated cells were compared (Fig. 4). Treatment of HL-60 cells with Am80 and PA024 suppressed cell growth [19] and, in accordance with this, also suppressed the expression of *c-myc*. In contrast, the expressions of *phosphoinositide-3-kinase, β-catalytic subunit* and *ribosomal protein S6 kinase polypeptide 1* were not suppressed by simultaneous stimulation of RAR by Am80 and RXR by PA024. The addition of 9-*cis* RA alone into the culture medium also showed the same gene expression patterns (data not shown). These results indicated that the difference observed in HL-60 cells treated with ATRA and Am80 was not caused by contamination of 9-*cis* RA.

4. Discussion

In this report, we firstly tried to identify the genes whose expressions were differentially modulated by ATRA and Am80 in HL-60 cells during a culture period of 72 h by a

Table 1
List of genes differentially modulated by ATRA and Am80

Set	Identifier	Title	Cell proliferation	Anti-apoptotis
36	S67334	**Phosphoinositide-3-kinase, catalytic, beta polypeptide**	GO[a]: 74; regulation of cell cycle	
	X85753	Cyclin-dependent kinase 8	GO: 74; regulation of cell cycle	
	L07540	Replication factor C (activator 1) 5, 36.5 kDa	GO: 6260; DNA replication	
	AB000450	Vaccinia related kinase 2	[12]	
	AL079273	Dead box protein 73D-like		
	M83822	LPS-responsive vesicle trafficking, beach and anchor containing		
	U33429	Potassium voltage-gated channel, shaker-related subfamily, beta member 2		
	U82328	E3-binding protein		
	AC004472	Hypothetical protein FLJ11560		
	HG1139–HT4910	N/A		
39	M60725	**Ribosomal protein S6 kinase, 70 kDa, polypeptide 1**	[13]	
	L19161	Eukaryotic translation initiation factor 2, subunit 3 gamma, 52 kDa	GO: 6414; translational elongation	
	X98743	DEAD/H (Asp-Glu-Ala-Asp/His) box polypeptide 18 (Myc-regulated)		
	D25547	Protein-L-isoaspartate (D-aspartate) *O*-methyltransferase		
	D30037	Phosphotidylinositol transfer protein, beta		
	M28209	RAB1A, member RAS oncogene family		
	U40462	Zinc finger protein, subfamily 1A, 1 (Ikaros)		
	W27675	Eukaryotic translation initiation factor 2A eIF2a		
	X17576	NCK adaptor protein 1		
	Z85986	Hypothetical protein MGC14254		
	AA013087	Homo sapiens, clone MGC: 17296 IMAGE: 3460701, mRNA, complete cds		
47	J04088	Topoisomerase (DNA) II alpha 170 kDa	GO: 6259; DNA metabolism	
	X76770	Poly(A) polymerase alpha	GO: 6350; transcription, [14]	
	X15331	Phosphoribosyl pyrophosphate synthetase 1	GO: 9165; nucleotide biosynthesis	
	AL080127	Tumor necrosis factor receptor superfamily, member 6b, decoy		GO: 6916; anti-apoptosis
	W28869	Testis enhanced gene transcript (BAX inhibitor 1)		[15]
	X63753	SON DNA binding protein		GO: 6916; anti-apoptosis
	AL049758	Protein kinase C and casein kinase substrate in neurons 2		
	X97544	Translocase of inner mitochondrial membrane 17 homolog A (yeast)		
	AB029032	Hypothetical protein KIAA1109		
	H15872	Hypothetical protein H41		
	AA189161	CGI-150 protein		
	U08997	Homo sapiens, clone MGC: 13241 IMAGE: 4026312, mRNA, complete cds		
40	U22376	v-myb myeloblastosis viral oncogene homolog (avian)	[16]	
	V00568	v-myc myelocytomatosis viral oncogene homolog (avian)	GO: 8283; cell proliferation;	
	U10564	WEE1 homolog (S. pombe)	GO: 74; regulation of cell cycle	
	U52960	SRB7 suppressor of RNA polymerase B homolog (yeast)	[17]	
	Z46376	Hexokinase 2	GO: 74; regulation of cell cycle	
	U29185	Prion protein (p27-30)		

Table 1 (*Continued*)

Set	Identifier	Title	Cell proliferation	Anti-apoptotis
	X98296	Ubiquitin specific protease 9, X chromosome (fat facets-like Drosophila)		
	AJ132440	Putative DNA/chromatin binding motif		
	Z24724	Hypothetical protein FLJ20986		
	M14219	N/A		
	HG3523-HT4899	N/A		

[a] GO: onthology defined by gene onthology consortium (http://www.godatabase.org/htdocs/docs.html).

large-scale analysis of the gene expression using a DNA microarray. By selecting genes whose expressions were changed by either ATRA or Am80 with statistical significance at least at one time point and whose expressions were reproducible through the time course, 610 genes out of 12,559 genes were left as the candidates. Next, we applied hierarchical and *k*-mean clustering algorithms to the time course expression data of these 610 genes. As the result, one-third of these genes (204 genes) were selected as the differentially controlled genes, while two-thirds of genes behaved similarly by both retinoid treatments. This fact suggested that the existence of (at least) two kinds of pathways which regulate HL-60 cell growth and differentiation, one is controlled specifically by ATRA (see below), and the other is by both retinoids.

Time course experiments involve multiple points and clustering is an algorithm that clarifies the patterns of gene expression. Since the pattern is dependent on not just one time point but on many, our analysis essentially represents the repetition of several assays and is more reproducible compared to a one time point type experiment, such as by treating HL-60 cells with either ATRA or Am80 for a certain period and then selecting differentially controlled genes at that point. Actually, the changes of the gene expression patterns induced by ATRA and Am80 were

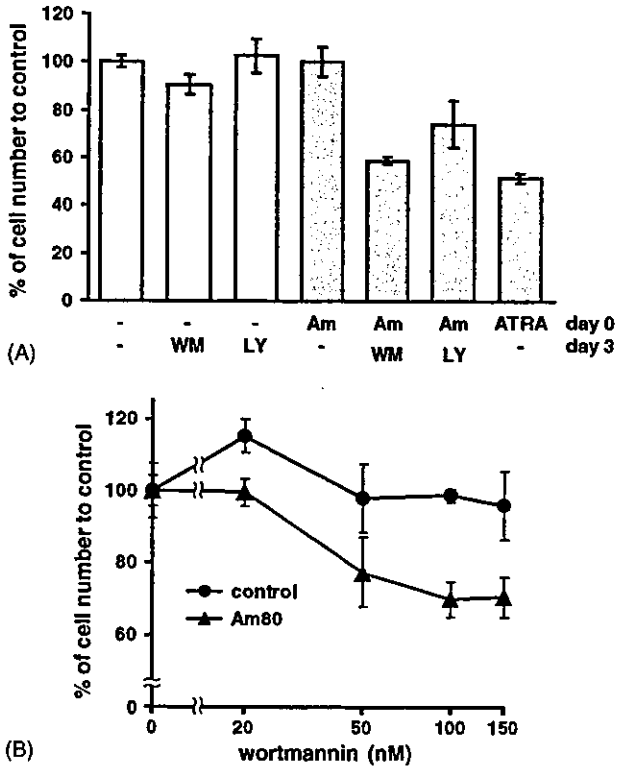

Fig. 3. Effect of PI3-kinase inhibitors on the growth of HL-60 cells treated with Am80. (A) Open bars: after 3 day culture of HL-60 cells without Am80, ethanol (−), wortmannin (WM), or LY294002 (LY) was added into the culture medium and the cells were cultured one more day before counting the number of the cells. Relative cell number is depicted as the number of cells in control (−, −) sets 100%. Each experiment was done in triplicate and error bar indicates standard error. Gray bars: same inhibitor treatments were done with HL-60 cells treated with Am80 for 3 days. The relative cell number is depicted as the number of cells in control (Am, −) sets 100%. Each experiment was done in triplicate. The relative number of HL-60 cells treated with ATRA for 4 days without inhibitors is also shown with that of the control experiments to (Am, −). (B) Different concentrations of wortmannin were added same as (A) and the number of the cells were counted. The relative cell number is depicted as the number of cells in control sets 100%. Each experiment was done in triplicate and error bar indicates standard error.

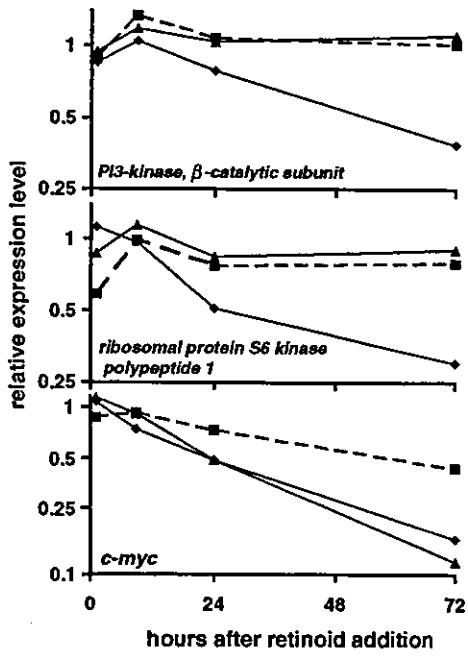

Fig. 4. Effects of RXR stimulation on the expressions of *phosphoinositide-3-kinase, β-catalytic subunit, ribosomal protein S6 kinase polypeptide 1*, and *c-myc*. RXR in HL-60 cells was stimulated by PA024 (retinoid synergist, [9]) with Am80 and the time courses of the expression levels of the three genes were measured by Affymetrix human genome U95A GeneChip. The relative expression levels were plotted: Am80 + PA024, (▲); ATRA (◆); and Am80 alone (■).

almost identical in two-thirds of the sets generated by *k*-mean clustering (Fig. 2A). This result depicted the high reproducibility of the clustering method clearly, which is why we chose the clustering of the time course data instead of analyzing the expression data of a given fixed time point.

4.1. Biological characteristics of genes differentially modulated by ATRA and Am80

The 204 genes, which were differentially modulated by ATRA and Am80, were important for the elucidation of the different effects of ATRA and Am80. Among them, the genes included in sets 36, 39, 40, and 47, which comprised a node in the hierarchical clustering, were interesting because their expressions were suppressed only by ATRA (Fig. 2) and many of them were related to cell proliferation or anti-apoptosis (Table 1). Cell proliferation is thought to be conducted by the cooperative regulation of signal transduction cascades. Taking a closer look into Table 1, three hierarchical relationships were found: (a) *DEAD/H box polypeptide 18* was regulated by *c-myc* [20]; (b) *topoisomerase (DNA) II alpha*170 kDa was a *c-myb* target gene [21]; (c) two genes, *phosphoinositide-3-kinase, β-catalytic subunit* and *ribosomal protein S6 kinase polypeptide 1*, were involved in the PI3-kinase/Akt signal transduction pathway [13,18]. The first two are relationships between transcription factors (*c-myc* and *c-myb*) and the regulated genes (*DEAD/H box polypeptide 18* and *topoisomerase (DNA) II alpha*170 kDa). Our previous study combining DNA microarray analyses with biomolecular-functional network analyses [22] indicated that the existence of such a kind of relationship implied that the behaviors of the genes were not caused by false positive signals. The third one is more interesting than the others in the context of cell growth, since the PI3-kinase/Akt pathway is positioned immediately downstream of the cell surface growth factor receptors [13,18]. Thus, modulation of this cascade triggers a change of the cell growth directly, while alterations in the expressions of the other two might be the downstream events of this cascade. The modulations of some other genes involved in this group, such as *replication factor C (activator 1) 5, eukaryotic translation initiation factor 2, subunit 3 gamma, poly(A) polymerase alpha*, etc., were also thought to be the downstream events of PI3-kinase/Akt pathway, however, this remains to be clarified.

The uniqueness of the modulation of the two genes involved in the PI3-kinase/Akt pathway by ATRA was also demonstrated by the experiment in which RXR–RAR heterodimer was stimulated simultaneously with PA024 and Am80 (Fig. 4). Activation of the genes downstream of the RAR–RXR heterodimer caused cell growth arrest and apoptosis [23]. The expression of *c-myc* was suppressed in this case, but on the other hand, the expressions of *phosphoinositide-3-kinase, β-catalytic subunit* and *ribosomal protein S6 kinase polypeptide 1* remained unchanged. These changes indicate that the expressions of *phosphoinositide-3-kinase, β-catalytic subunit* and *ribosomal protein S6 kinase polypeptide 1* were uniquely suppressed by ATRA treatment.

4.2. Role of PI3-kinase/Akt pathway in the late stage of HL-60 cell differentiation

Several studies have been already reported concerning the relationship between PI3-kinase and HL-60 cell differentiation [24–27]. However, there are few reports that discuss the PI3-kinase activity and HL-60 cell proliferation during differentiation [28,29]. According to a report by Liu et al. [28], when HL-60 cells cultured in serum free medium were treated with ATRA, they differentiated poorly and underwent apoptosis. However, the addition of IGF-I, which induced PI3-kinase activity in the cells, prevented the apoptosis and increased the differentiated cell population. These results indicated that keeping PI3-kinase active is a prerequisite for the cell proliferation during the HL-60 cell differentiation process. According to our gene expression analyses, the expressions of two components belonging to the PI3-kinase/Akt pathway, *phosphoinositide-3-kinase, β-catalytic subunit* and *ribosomal protein S6 kinase polypeptide 1*, were suppressed only in ATRA-treated HL-60 cells but not in Am80-treated cells. Taking the results by Liu et al. into consideration, the different expression patterns of these two genes should explain the different effects of ATRA and Am80 on the HL-60 cell proliferation during the differentiation process, that is, ATRA suppresses HL-60 cell proliferation more effectively than Am80. If the different modulation of the expression of the two components of the PI3-kinase/Akt pathway were the main cause of the difference in the HL-60 cell growth suppression by ATRA and Am80, inhibition of this pathway in an alternative way might be enough to induce the cell growth suppression in Am80-treated HL-60 cells. To examine this hypothesis, wortmannin and LY294002, well known PI3-kinase inhibitors, were added to the HL-60 cells treated with Am80 for 3 days and the change in the cell growth was assayed 1 day later. Both inhibitors inhibited the cell growth at a concentration that did not suppress the growth of cells cultured without Am80 (Fig. 3) in a dose-dependent manner. This result meant that the inhibition of PI3-kinase alone was able to suppress the cell growth of the Am80-treated HL-60 cells and indicated that modulation of the PI3-kinase/Akt pathway was important in the cell growth control during the HL-60 cell differentiation induced by retinoids. A recent report by Ma et al. [29] supported this idea. In that report, they suggested that the survival of differentiated HL-60 cells induced by ATRA depends on the ability of the PI3-kinase pathway. The mechanism that explains why only ATRA suppressed the expressions of *phosphoinositide-3-kinase, β-catalytic subunit* and *ribosomal protein S6 kinase polypeptide 1* remains to be clarified.

In our case, neither inhibitor affected the HL-60 cell differentiation (data not shown). In experiments dealing with the relationship between PI3-kinase and HL-60 cell differentiation, when PI3-kinase inhibitors were used to assess the involvement of PI3-kinase activity, they were added to the culture several hours before or at the same time as the retinoid treatment [24–27]. In contrast, both inhibitors were added to the culture medium 3 days after the Am80 treatment in our study. It is plausible that the commitment of HL-60 cell differentiation into granulocytes was already established during the 3 day treatment with Am80, thus the inhibition of PI3-kinase showed no effect on the HL-60 cell differentiation.

4.3. Clinical potential of concomitant usage of Am80 and PI3-kinase inhibitors

As shown in the result section, we were able to mimic the effects of ATRA on HL-60 cell proliferation by using PI3-kinase inhibitors in Am80-treated cells (Fig. 3). This would be clinically important because the concomitant use of synthetic retinoids and PI3-kinase inhibitors has the potential to widen their activities with fewer side-effects. For example, inhibitors of PI3-kinase might help to attain complete remission in patients who do not respond to Am80 well, because the inhibitors should inhibit the proliferation of Am80-treated cells. Another possibility is the case of solid tumor treatment. PI3-kinase activity has been linked to a variety of human tumors including breast cancer, lung cancer, melanomas and so on [18]. Thus, inhibitors of PI3-kinase activity are promising as novel chemotherapeutic agents. The application of synthetic retinoids to solid tumors has also been tried, particularly Am555S (TAC-101), another synthetic retinoid of the benzanilide series [30]. It is interesting that our results are applicable to such cases, which may thus expand the use of retinoids for cancer treatment.

Acknowledgements

We thank Chie Knudsen for kind help with preparation of the supplemental table. This work was supported by Program for Promotion of Fundamental Studies in Health Sciences (MF-16 and MPJ-6) of the Organization for Pharmaceutical Safety and Research of Japan.

References

[1] Zhang J-W, Gu J, Wang Z-Y, Chen S-J, Chen Z. Mechanisms of all-*trans* retinoic acid-induced differentiation of acute promyelocytic leukemia cells. J Biosci 2000;25:275–84.

[2] Tobita T, Takeshita A, Kitamura K, Ohnishi K, Yanagi M, Hiraoka A, et al. Treatment with a new synthetic retinoid, Am80, of acute promyelocytic leukemia relapsed from complete remission induced by all-*trans* retinoic acid. Blood 1997;90:967–73.

[3] Takeuchi M, Yano T, Omoto E, Takahashi K, Kibata M, Shudo K, et al. Relapsed acute promyelocytic leukemia previously treated with all-*trans* retinoic acid: clinical experience with a new synthetic retinoid, Am-80. Leuk Lymphoma 1998;31:441–51.

[4] Kagechika H. Novel synthetic retinoids and separation of the pleiotropic retinoidal activities. Curr Med Chem 2002;9:591–608.

[5] Ishida S, Shudo K, Takada S, Koike K. A direct role of transcription factor E2F in *c-myc* gene expression during granulocytic and macrophage-like differentiation of HL60 cells. Cell Growth Differ 1995;6:229–37.

[6] Hashimoto Y, Kagechika H, Kawachi E, Shudo K. Specific uptake of retinoids into human promyelocytic leukemia cells HL-60 by retinoid-specific binding protein: possibly the true retinoid receptor. Jpn J Cancer Res 1988;79:473–83.

[7] Hashimoto Y, Petkovich M, Gaub MP, Kagechika H, Shudo K, Chambon P. The retinoic acid receptors alpha and beta are expressed in the human promyelocytic leukemia cell line HL-60. Mol Endocrinol 1989;3:1046–52.

[8] Kagechika H, Kawachi E, Hashimoto Y, Shudo K. Retinobenzoic acid 2. Structure-activity relationships of chalcone-4-carboxylic acids and falvone-4′-carboxylic acids. J Med Chem 1989;32:834–40.

[9] Ohta K, Kawachi E, Inoue N, Fukasawa H, Hashimoto Y, Itai A, et al. Retinoidal pyrimidinecarbosylic acids. Unexpected diaza-substituent effects in retinobenzoic acids. Chem Pharm Bull Tokyo 2000;48:1504–13.

[10] Toda K, Ishida S, Nakata K, Matsuda R, Shigemoto-Mogami Y, Fujishita K, et al. Test of significant differences with *a priori* probability in microarray experiments. Anal Sci 2003;19:1529–35.

[11] Balmer JE, Blomhoff R. Gene expression regulation by retinoic acid. J Lipid Res 2002;43:1773–808.

[12] Lopez-Borges S, Lazo PA. The human vaccinia-related kinase 1 (VRK1) phosphorylates threonine-18 within the mdm-2 binding site of the p53 tumor suppressor protein. Oncogene 2000;19:3656–64.

[13] Pullen N, Thomas G. The modular phosphorylation and activation of $p70^{s6k}$. FEBS Lett 1997;410:78–82.

[14] Lucchini R, Vezzoni P, Giardini R, Vezzoni MA, Raineri M, Clerici L. Poly(A) polymerase distribution in normal and malignant lymphoid cells. Tumori 1984;70:141–6.

[15] Xu Q, Reed JC. Bax inihibitor-1, a mammalian apoptosis suppressor identified by functional screening in yeast. Mol Cell 1998;1:337–46.

[16] Oh IH, Reddy EP. The myb gene family in cell growth, differentiation and apoptosis. Oncogene 1999;18:3017–33.

[17] Maldonado E, Shiekhattar R, Sheldon M, Cho H, Drapkin R, Rickert P, et al. A human RNA polymerase II complex associated with SRB and DNA-repair proteins. Nature 1996;381:86–9.

[18] Chang F, Lee JT, Navolanic PM, Steelman LS, Shelton JG, Blalock WL, et al. Involvement of PI3K/Akt pathway in cell cycle progression, apoptosis, and neoplastic transformation: a target for cancer chemotherapy. Leukemia 2003;17:590–603.

[19] Ishida S, Shigemoto-Mogami Y, Kagechika H, Shudo K, Ozawa S, Sawada J, et al. Clinically potential subclasses of retinoid synergists revealed by gene expression profiling. Mol Cancer Ther 2003;2:49–58.

[20] Grandori C, Mac J, Siebelt F, Ayer DE, Eisenman RN. Myc–Max heterodimers activate a *DEAD box* gene and interact with multiple E box-related sites in vivo. EMBO J 1996;15:4344–57.

[21] Brandt TL, Fraser DJ, Leal S, Halandras PM, Kroll AR, Kroll DJ. c-Myb *trans*-activates the human DNA topoisomerase II alpha gene promoter. J Biol Chem 1997;272:6278–84.

[22] Toda K, Ishida S, Nakata K, Matsuda R, Shigemoto-Mogami Y, Ozawa S, et al. Improvement in reliability of probabilistic test of significant differences in genechip experiments. Anal Sci 2004;20:731–3.

[23] Nagy L, Thomazy VA, Shipley GL, Fesus L, Lamph W, Heyman RA, et al. Activation of retinoid X receptors induces apoptosis in HL-60 cell lines. Mol Cell Biol 1995;15:3540–51.

[24] Marcinkowska E, Wiedlocha A, Radzikowski C. Evidence that phosphatidylinositol 3-kinase and $p70^{S6K}$ protein are involved in differ-

entiation of HL-60 cells induced by calcitriol. Anticancer Res 1998;18:3507–14.
[25] Marchisio M, Bertagnolo V, Colamussi ML, Capitani S, Neri LM. Phospatidylinositol 3-kinase in HL-60 nuclei is bound to the nuclear matrix and increases during granulocytic differentiation. Biochem Biophys Res Comm 1998;253:346–51.
[26] Bertagnolo V, Neri LM, Marchisio M, Mischiati C, Capitani S. Phosphoinositide 3-kinase activity is essential for all-*trans*-retinoic acid-induced granulocytic differentiation of HL-60 cells. Cancer Res 1999;59:542–6.
[27] Capitani S, Marchisio M, Neri LM, Brugnoli F, Gonelli A, Bertagnolo V. Phosphoinositide 3-kinase is associated to the nucleus of HL-60 cells and is involved in their ATRA-induced granulocytic differentiation. Eur J Histochem 2000;44:61–5.
[28] Liu Q, Schacher D, Hurth C, Freund GG, Dantzer R, Kelley KW. Activation of phosphatidylinositol 3′-kinase by insulin-like growth factor-I rescues promyeloid cells from apoptosis and permits their differentiation into granulocytes. J Immun 1997;159:829–37.
[29] Ma J, Liu Q, Zeng YX. Inhibition of phosphatidylinositol 3-kinase causes apoptosis in retinoic acid differentiated HL-60 leukemia cells. Cell Cycle 2004;3:67–70.
[30] Hashimoto Y. Structural development of synthetic retinoids and thalidomide-related molecules. Cancer Chemother Pharmacol 2003; 52:S16–23.

Ca^{2+} waves in keratinocytes are transmitted to sensory neurons: the involvement of extracellular ATP and $P2Y_2$ receptor activation

Schuichi KOIZUMI*, Kayoko FUJISHITA†, Kaori INOUE‡, Yukari SHIGEMOTO-MOGAMI†, Makoto TSUDA† and Kazuhide INOUE†§[1]

*Division of Pharmacology, National Institute of Health Sciences, 1-18-1 Kamiyoga, Setagaya, Tokyo 158-8501, Japan, †Division of Biosignaling, National Institute of Health Sciences, 1-18-1 Kamiyoga, Setagaya, Tokyo 158-8501, Japan, ‡Shiseido Research Center, 2-12-1 Fukuura, Kanazawa-ku, Yokohama 236-8643, Japan, and §Graduate School of Pharmaceutical Sciences, Kyushu University, 3-1-1 Maidashi, Fukuoka 812-8582, Japan

ATP acts as an intercellular messenger in a variety of cells. In the present study, we have characterized the propagation of Ca^{2+} waves mediated by extracellular ATP in cultured NHEKs (normal human epidermal keratinocytes) that were co-cultured with mouse DRG (dorsal root ganglion) neurons. Pharmacological characterization showed that NHEKs express functional metabotropic $P2Y_2$ receptors. When a cell was gently stimulated with a glass pipette, an increase in $[Ca^{2+}]_i$ (intracellular Ca^{2+} concentration) was observed, followed by the induction of propagating Ca^{2+} waves in neighbouring cells in an extracellular ATP-dependent manner. Using an ATP-imaging technique, the release and diffusion of ATP in NHEKs were confirmed. DRG neurons are known to terminate in the basal layer of keratinocytes. In a co-culture of NHEKs and DRG neurons, mechanical-stimulation-evoked Ca^{2+} waves in NHEKs caused an increase in $[Ca^{2+}]_i$ in the adjacent DRG neurons, which was also dependent on extracellular ATP and the activation of $P2Y_2$ receptors. Taken together, extracellular ATP is a dominant messenger that forms intercellular Ca^{2+} waves in NHEKs. In addition, Ca^{2+} waves in NHEKs could cause an increase in $[Ca^{2+}]_i$ in DRG neurons, suggesting a dynamic cross-talk between skin and sensory neurons mediated by extracellular ATP.

Key words: ATP, Ca^{2+} wave, cross-talk, dorsal root ganglion neuron, keratinocyte, $P2Y_2$ receptor.

INTRODUCTION

The skin is the largest organ of the body and is exposed to multiple external stimuli. It protects water-rich internal organs from harmful environmental factors such as dryness, chemicals, noxious heat and UV irradiation. In addition, the skin is exposed to various substances such as ATP, bradykinin and histamine after skin injury and during inflammatory skin diseases and allergic reactions respectively. Thus the skin expresses various sensors for environmental stimuli [1,2] or neurotransmitters [3–6]. Various environmental stimuli or neurotransmitters often cause changes in $[Ca^{2+}]_i$ (intracellular Ca^{2+} concentration) in the skin [5,7,8]. Ca^{2+} dynamics play an important role in the homoeostasis of the skin epidermis, the outermost part of skin tissue; the skin epidermis tunes the balance between the proliferation and differentiation of epidermal keratinocytes [1,9].

Propagation of intercellular Ca^{2+} waves from one cell to another is a well-known phenomenon in non-excitable cells such as astrocytes [10,11], hepatocytes [12], epithelial cells [13] and endothelial cells [14]. These cells lack regenerative electrical action potentials but use Ca^{2+} waves for their long-range communications. In astrocytes, extracellular molecules such as glutamate [11] and ATP [15], rather than gap junction via connexin43, have been suggested to be important factors for the Ca^{2+} wave [16]. Epidermal keratinocytes are non-excitable cells and do not produce action potentials. However, the mechanisms of intercellular Ca^{2+} waves in keratinocytes have received only limited attention. Given that Ca^{2+} waves in keratinocytes are mediated by the release of extracellular molecules, such signals may also affect the activity of surrounding cells such as sensory neurons. Although junctions have not been found between keratinocytes and sensory termini, ultrastructural studies have shown that keratinocytes contact DRG (dorsal root ganglion) nerve fibres through membrane–membrane apposition [17,18]. Immunostaining of the neuronal marker PGP 9.5 (protein gene product 9.5) revealed the presence of free nerve endings at epidermal keratinocytes [19]. There is indirect evidence that keratinocytes communicate with sensory neurons via extracellular molecules. For example, although dissociated DRG neurons can be directly activated by heat and cold, warm responses have only been demonstrated in experiments where skin–nerve connectivity is intact [20,21]. A warmth sensor, TRPV3, is present in epidermal keratinocytes, but not in sensory neurons [19]. Sensory neurons themselves sense various external stimuli, but there might be skin-derived regulatory mechanisms by which sensory signalling is modulated.

In the present study, we report that mechanical stimulation of NHEKs (normal human epidermal keratinocytes) with a glass pipette induces propagating Ca^{2+} waves in an extracellular ATP-dependent manner. NHEKs release ATP and, in turn, the released ATP activates $P2Y_2$ receptors in NHEKs. We also demonstrate that, in a co-culture of NHEKs and DRG neurons, such extracellular ATP-dependent Ca^{2+} waves in NHEKs cause increases in $[Ca^{2+}]_i$ even in the adjacent DRG neurons, suggesting that dynamic cross-talk occurs between keratinocytes and DRG neurons via extracellular ATP.

EXPERIMENTAL

Cell culture

NHEKs were obtained as cryopreserved first passage cells from neonatal foreskins (Kurabo, Osaka, Japan). Cells were plated on collagen-coated coverslips and then cultured in serum-free

Abbreviations used: ATPγS, adenosine 5′-[γ-thio]triphosphate; BSS, balanced salt solution; $[Ca^{2+}]_i$, intracellular Ca^{2+} concentration; DRG, dorsal root ganglion; αβmeATP, α,β-methylene-ATP; 2meSADP, 2methyl-thio-ADP; NHEK, normal human epidermal keratinocyte; RT, reverse transcriptase.

[1] To whom correspondence should be addressed (e-mail inoue@nihs.go.jp).

keratinocyte growth medium consisting of Humedia-KB2 (Kurabo), supplemented with bovine pituitary extract (0.4 %, v/v), human recombinant epidermal growth factor (0.1 ng/ml), insulin (10 μg/ml), cortisol (0.5 μg/ml), gentamicin (50 μg/ml) and amphotericin B (50 ng/ml). The media were replaced every 2–3 days. For co-culturing NHEKs and mouse DRG neurons, NHEKs were seeded on mitomycin C (4 μg/ml)-treated 3T3-J2 fibroblast feeder layers (2×10^5 cells/cm^2) in 'Green' medium [3:4 Dulbecco's minimal Eagle's medium and 1:4 Ham's F12, supplemented with 10 % (v/v) foetal bovine serum, 20 mM Hepes, 100 units/ml penicillin, 100 μg/ml streptomycin, 5 μg/ml insulin, 0.5 μg/ml cortisol, 0.1 nM cholera enterotoxin, 0.01 μg/ml recombinant human epidermal growth factor, 0.25 μg/ml amphotericin B and 180 μM adenine]. The dissociated mouse DRG neurons were seeded, 2 days after the seeding of NHEKs, on the cell layer and then cultured for an additional 1 week.

Ca^{2+} imaging in single NHEKs

Changes in $[Ca^{2+}]_i$ in single cells were measured by the fura 2 method as described by Grynkiewicz et al. [22] after minor modifications [23]. In brief, the culture medium was replaced with BSS (balanced salt solution) of the following composition (mM): NaCl 150, KCl 5.0, $CaCl_2$ 1.8, $MgCl_2$ 1.2, Hepes 25 and D-glucose 10 (pH 7.4). Cells were loaded with fura 2 by incubation with 5 μM fura 2/AM (fura 2 acetoxymethyl ester; Molecular Probes, Eugene, OR, U.S.A.) at room temperature (20–22 °C) in BSS for 45 min, followed by washing with BSS and a further 15 min incubation to allow de-esterification of the loaded dye. The coverslips were mounted on an inverted epifluorescence microscope (TMD-300; Nikon, Tokyo, Japan) equipped with a 75 W xenon lamp and band-pass filters of 340 and 360 nm wavelengths. Measurements were carried out at room temperature. Images were recorded by a high-sensitivity silicon intensifier target camera (C-2741-08; Hamamatsu Photonics, Hamamatsu, Japan) and the image data were regulated by a Ca^{2+} analysing system (Furusawa Laboratory Appliance, Kawagoe, Japan). The absolute $[Ca^{2+}]_i$ was estimated from the ratio of emitted fluorescences (F_{340}/F_{360}) according to a calibration curve obtained by using Ca^{2+} buffers. For Ca^{2+}-free experiments, Ca^{2+} was removed from the BSS (0 Ca^{2+}). Drugs were dissolved in BSS and applied by superfusion. For mechanical stimulation, a single NHEK in the centre of the microscopic field was probed with a glass micropipette using a micromanipulator (Narishige, Tokyo, Japan). Under visible light, the tip of the micropipette was positioned approx. 2 μm over the cell to be stimulated. When sampling, the micropipette was rapidly lowered by approx. 2 μm and then rapidly returned to its original position. If the stimulated cell showed no increase in fluorescence, the pipette was lowered again until stimulation was seen. If the stimulated cell showed any sign of damage (dye leakage or abnormal morphology), the experiment was eliminated. For confocal Ca^{2+} imaging, the cells were loaded with 5 μM fura 4/AM for 30–40 min at room temperature and then mounted on a microscope (TE-2000; Nikon) equipped with a CSU-10 laser-scanning unit (Yokogawa, Tokyo, Japan) and a high-sensitivity CCD (charge-coupled-device) camera (ORCA-ER; Hamamatsu Photonics), as described previously [24]. To compensate for the uneven distribution of the fluo-4, self-ratios were calculated ($R_s = F/F_0$), which were subsequently converted into Ca^{2+} concentration using the following equation:

$$[Ca^{2+}]_i = R_s K_d / [(K_d / [Ca^{2+}]_{rest}) - R_s]$$

The K_d value of fluo-4 for NHEKs was taken to be 706 nM as determined by an *in vivo* calibration method.

Table 1 Primer pairs and end-products

Amplicon shows the base pairs of the PCR end-product.

Gene	Primer	Size (-mer)	Amplicon (bp)
P2Y1	F: 5′-GAGGGCCCGGCTTGATT-3′	17	67
	R: 5′-ATACGTGGCATAAACCCTGTCA-3′	22	
P2Y2	F: 5′-TGGTGCGCTTCCTCTTCTACA-3′	21	72
	R: 5′-ACCGGTGCACGCTGATG-3′	17	
P2Y4	F: 5′-TCATGGCTCGTCGCCTGTA-3′	19	67
	R: 5′-AGAGAGCGGAGGCGAGAAG-3′	19	
P2Y6	F: 5′-CCTGCCCACAGCCATCTT-3′	18	116
	R: 5′-CAGTGAGAGCCATGCCATAGG-3′	21	
P2Y11	F: 5′-CTGCCCTGCCAACTTCTTG-3′	19	78
	R: 5′-ACCAGTATGGGCCACAGGAA-3′	20	
P2Y12	F: 5′-CCTTTCCATTTTGCCCGAAT-3′	20	74
	R: 5′-GTATTTTCAGCAGTGCAGTCAAAGA-3′	25	

Imaging of ATP release

ATP release from NHEKs was detected with a luciferin–luciferase bioluminescence assay. After an initial 30 min superfusion period, superfusion was stopped and the cell chamber was filled with BSS containing a luciferase reagent (ATP bioluminescence assay kit CLS II; Roche Diagnostics, Mannheim, Germany). ATP bioluminescence was detected and visualized with a VIM camera (C2400-35; Hamamatsu Photonics) using an integration time of 30 s. The absolute ATP concentration was estimated using a standard ATP solution (ATP bioluminescence assay kit CLS II).

Immunocytochemistry

Cultures were fixed with 4 % (w/v) paraformaldehyde for 10 min and soaked in PBS solution. Cells were incubated with primary antibodies (rabbit anti-peripherin antibody, 1:200; Chemicon, Temecula, CA, U.S.A.; monoclonal mouse anti-cytokeratin14 antibody, 1:100; Cymbus Biotechnology, Chandlers Ford, U.K.), dissolved in blockace solution (1:10 dilution; Dainippon, Osaka, Japan) for 1 h at room temperature and then covered with diluted (1:500) secondary fluorescent antiserum solution (Alexa488- and Alexa546-conjugated rabbit and mouse anti-IgGs respectively) and kept at 4 °C overnight. Then, the cells were washed three times with PBS containing 0.05 % Tween 20 for 15 min and mounted with Vectashied (Vector Laboratories, Burlingame, CA, U.S.A.). Images were obtained by confocal microscopy (Radiance 2000; Bio-Rad Japan, Tokyo, Japan).

Reverse transcriptase (RT)–PCR of P2 receptors

The total RNA was isolated and purified using RNeasy mini kits (Qiagen) according to the manufacturer's instructions. RT–PCR amplifications were performed using Taqman One-step RT–PCR Master Mix Reagents and 200 nM of each P2 receptor-specific primer. Using the software Primer Express (Applied Biosystems, Tokyo, Japan), clone-specific primers were designed to recognize human P2Y receptors, as shown in Table 1. All primers had similar melting temperatures for running the same cycling programme for all samples. RT–PCR was performed by 30 min reverse transcription at 48 °C, 10 min AmpliTaq Gold activation at 95 °C, then 15 s denaturation at 95 °C and, finally, 1 min annealing and elongation at 60 °C for 40 cycles in a PRISM 7700 (Applied Biosystems). To exclude contamination by unspecific PCR products such as primer dimers, melting curve analysis was performed on all the final PCR products after the cycling procedure.

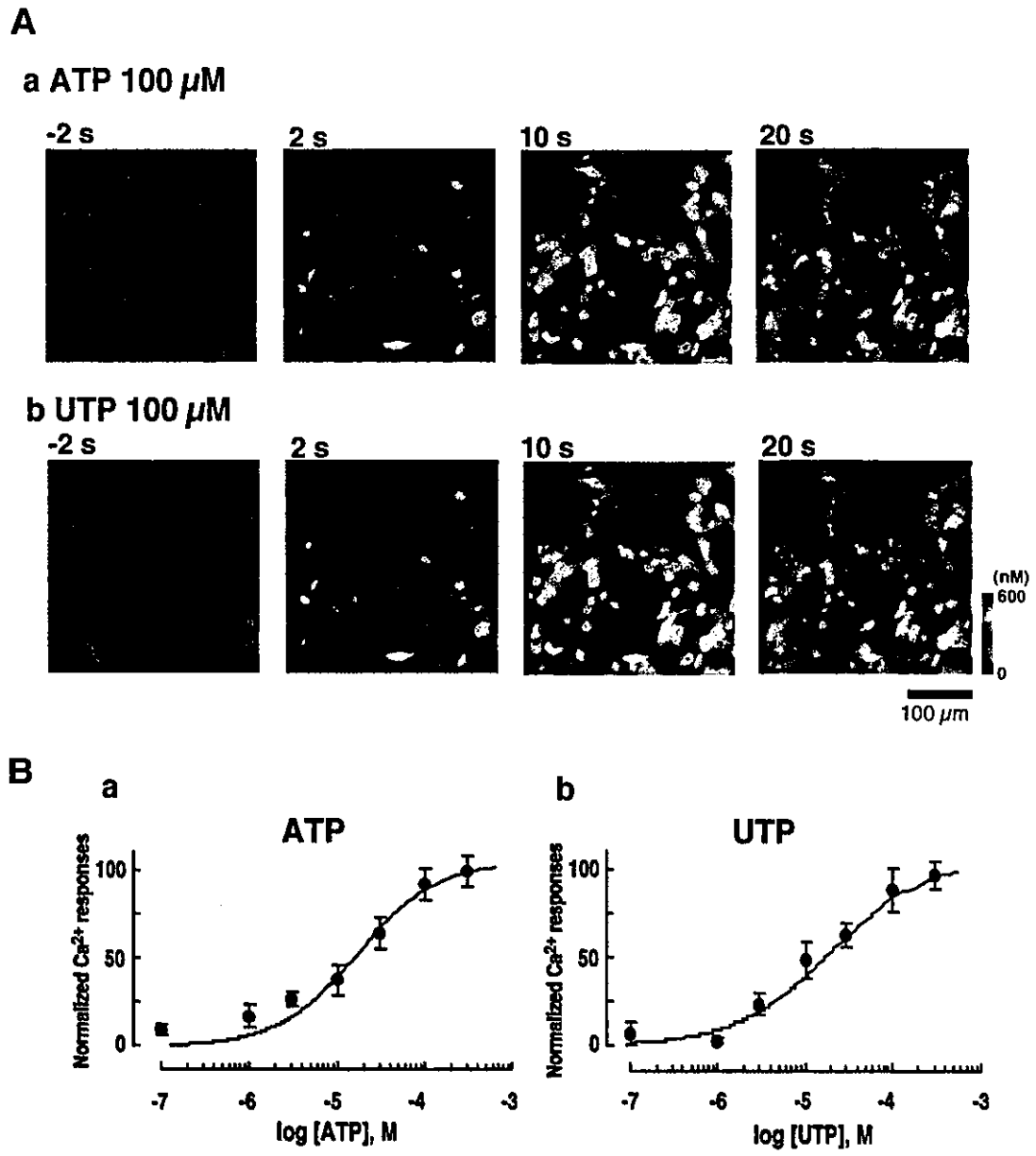

Figure 1 Increases in $[Ca^{2+}]_i$ evoked by both applied ATP and UTP in NHEKs

(**A**) Sequential pseudo colour images of Ca^{2+} responses to 100 μM ATP (**a**) and UTP (**b**). Images were obtained from a confocal laser microscope, showing self-ratios of fluo-4 fluorescence. Images were recorded 2 s before (−2 s) and 2, 10 and 20 s after ATP or UTP application. (**B**) Concentration–response curves for (**a**) ATP- and (**b**) UTP-evoked increases in $[Ca^{2+}]_i$ in NHEKs. Increases in $[Ca^{2+}]_i$ in NHEKs were monitored by ratiometric fura 2 fluorescence ($\Delta F_{340}/F_{360}$) and were then converted into absolute value of $[Ca^{2+}]_i$ using a standard calibration curve. The maximum $[Ca^{2+}]_i$ increase was observed when cells were stimulated with 300 μM ATP (**a**) or UTP (**b**). The increase in $[Ca^{2+}]_i$ at each ATP or UTP concentration was normalized by the maximum increase in $[Ca^{2+}]_i$. Results are the means ± S.E.M. for 28–73 cells tested. Both the ATP- and UTP-evoked concentration–response curves were almost identical with the ED_{50} values of 21 and 20 μM respectively.

Statistics

Experimental results are expressed as means ± S.E.M. and statistical differences between two groups were determined by Student's *t* test.

RESULTS

Characterization of ATP-evoked $[Ca^{2+}]_i$ increases in NHEKs

Exogenously applied ATP induced an increase in $[Ca^{2+}]_i$ in NHEKs with an ED_{50} value of 21 μM (Figures 1Aa and 1Ba). UTP also caused an increase in $[Ca^{2+}]_i$ in the cells, with a similar ED_{50} value of 20 μM (Figures 1Ab and 1Bb). The ATP-evoked increase in $[Ca^{2+}]_i$ was almost independent of the extracellular Ca^{2+}, but was decreased by U73122, an inhibitor of phospholipase C, and thapsigargin, an inhibitor of Ca^{2+}-ATPase of Ca^{2+} stores, suggesting the involvement of inositol 1,4,5-trisphosphate/phospholipase C-linked metabotropic P2Y receptors in the Ca^{2+} responses (Figure 2A). UTP activates UTP-preferring $P2Y_2$ and $P2Y_4$ receptors, and UDP, generated by de-phosphorylation of UTP, stimulates $P2Y_6$ receptors. We therefore analysed the expression of mRNAs for these P2Y receptors using an RT–PCR method and detected the signals for $P2Y_1$, $P2Y_2$ and $P2Y_{11}$ receptors (Figure 2B, inset). Each PCR product possessed the predicted length (Table 1). Signals for $P2Y_4$, $P2Y_6$ and $P2Y_{12}$ were hardly detected in NHEKs. To confirm the functional responses

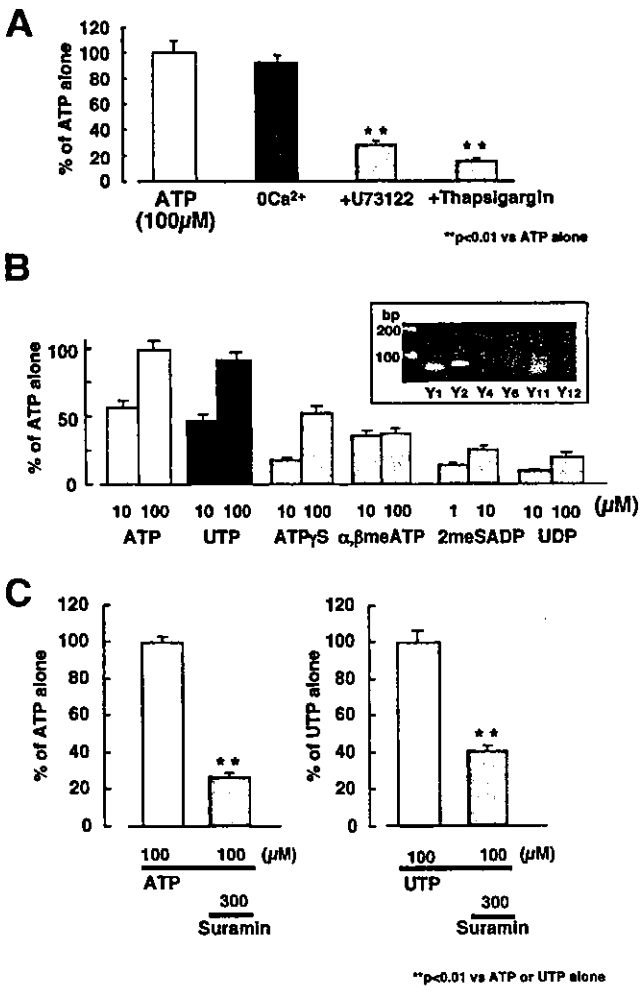

Figure 2 Characterization of P2 receptor-mediated Ca^{2+} responses in NHEKs

The ATP-evoked increases in $[Ca^{2+}]_i$ in NHEKs were characterized. Increases in $[Ca^{2+}]_i$ in cells were calculated by ratiometric fura 2 fluorescence ($\Delta F_{340}/F_{360}$) and a standard calibration curve. Values were normalized by the Ca^{2+} response at 100 μM ATP or UTP and were expressed as a percentage of ATP or UTP alone (**C**, right). (**A**) ATP was applied to NHEKs for 20 s and the U73122 (5 μM) was applied to the cells 10 min before and during the ATP application. Thapsigargin (100 nM) was applied to the cells 5 min before and during the ATP application. Results were obtained from 28 to 61 cells tested (at least two independent experiments). $^{**}P < 0.01$, significant differences from the response evoked by ATP alone. (**B**) Pharmacological characterization of Ca^{2+} responses in NHEKs. UTP was as potent as ATP. ATPγS and $\alpha\beta$meATP were much less potent than ATP. 2meSADP and UDP caused only slight increases in $[Ca^{2+}]_i$ in NHEKs. Results were obtained from 24 to 57 cells tested (at least two independent experiments). The inset shows the agarose-gel electrophoresis, indicating expression of mRNAs for various P2Y receptors in NHEKs. (**C**) Suramin (300 μM) inhibited both the ATP- and UTP-evoked increases in $[Ca^{2+}]_i$ in NHEKs. Results were obtained from 117 to 126 cells tested (four independent experiments). $^{**}P < 0.01$, significant differences from the response evoked by ATP or UTP alone.

of these P2Y receptors, we further performed pharmacological analysis using the fura 2-based Ca^{2+} imaging methods. The increase in $[Ca^{2+}]_i$ evoked by UTP was almost identical with that evoked by ATP. Both the $P2Y_{11}$ receptor agonist ATPγS (adenosine 5′-[γ-thio]triphosphate) and the P2X receptor agonist $\alpha\beta$meATP (α,β-methylene-ATP) caused increases in $[Ca^{2+}]_i$, but they were less than those caused by ATP or UTP. 2meSADP (2methyl-thio-ADP), a $P2Y_1$ receptor agonist, and UDP, a $P2Y_6$ receptor agonist, evoked only slight increases in $[Ca^{2+}]_i$ in the cells. The potency rank order for the Ca^{2+} response was ATP = UTP > ATPγS > $\alpha\beta$meATP > 2meSADP > UDP (Figure 2B). Cross-desensitization was observed between ATP and UTP (results not shown). Suramin at 300 μM decreased both the ATP- and UTP-evoked $[Ca^{2+}]_i$ increases (Figure 2C: 29.8 ± 2.2 % of ATP alone, $n = 128$; 44.1 ± 2.7 % of UTP alone, $n = 117$). These results suggest that the $P2Y_2$ receptors were responsible for these responses.

Propagating Ca^{2+} waves in response to mechanical stimulation in NHEKs

When an NHEK was stimulated with a glass pipette, an increase in $[Ca^{2+}]_i$ in the cell was observed, followed by induction of a propagating Ca^{2+} wave after a time lag in neighbouring NHEKs (Figure 3A, upper panels). The findings that the same cell evoked a Ca^{2+} response to repeated (up to three times) mechanical stimulations (results not shown) and that the cell showed some sign of damage suggest that mechanical stimulation would not cause injury to the stimulated cells. The propagation of Ca^{2+} waves was abolished by 80 units/ml apyrase [grade III; Figures 3A (lower panels) and 3B]. Both the P2 receptor antagonists suramin (300 μM) and pyridoxal phosphate-6-azophenyl-2′,4′-disulphonic acid (100 μM) significantly inhibited the Ca^{2+} wave; however, adenosine 3′-phosphate 5′-phosphosulphate (100 μM), an antagonist to the $P2Y_1$ receptor, and 1-octanol (500 μM), an inhibitor of gap junction, did not affect the Ca^{2+} waves (Figure 3C). The $[Ca^{2+}]_i$ increase in the stimulated cells was not affected by these antagonists. All these findings suggest that the propagating Ca^{2+} wave in response to mechanical stimulation in NHEKs was mediated by extracellular ATP and mainly by the activation of $P2Y_2$ receptors.

Release and diffusion of ATP from NHEKs

To demonstrate directly the stimulus-evoked release of ATP from NHEKs, we modified the luciferin–luciferase chemiluminescence bioassay for detecting ATP levels by using a high-sensitivity single photon-counting camera to correlate photon counts with increases in extracellular ATP. NHEKs were bathed in a solution containing the luciferin–luciferase reagents and photons were counted before and 30 s after mechanical stimulation of an NHEK. Figure 4(a) shows a phase-contrast image of a microscopic field, and Figures 4(b) and 4(c) show bioluminescence images before and after mechanical stimulation in the same field respectively. The standard calibration curve obtained under this condition showed a high correlation between the bioluminescence intensity and the ATP concentration with a correlation coefficient of 0.986 over a concentration range of 10 nM–10 μM (Figure 4d). The resting level of the bioluminescence signal was very low; then, it was increased to a level sufficient to evoke increases in $[Ca^{2+}]_i$ in NHEKs (3.2 ± 0.91 μM, $n = 12$) in response to mechanical stimulation for 30 s (Figures 4c and 4f). To visualize the spatiotemporal dynamics of the stimulus-evoked release of ATP from NHEKs, the extracellular ATP levels were plotted as pseudo colour images using the Excel 2-D surface plot program. As shown in Figures 4(e) and 4(f), the levels of extracellular ATP after mechanical stimulation were highest at the site of stimulation and decreased concentrically. These results show that the mechanically evoked Ca^{2+} waves were well associated with the release of ATP from NHEKs and the activation of $P2Y_2$ receptors.

Ca^{2+} waves in NHEKs activate increase in $[Ca^{2+}]_i$ in DRG neurons

As described in the Introduction section, sensory neurons terminate in the skin. Hence, a co-culture of NHEKs and mouse

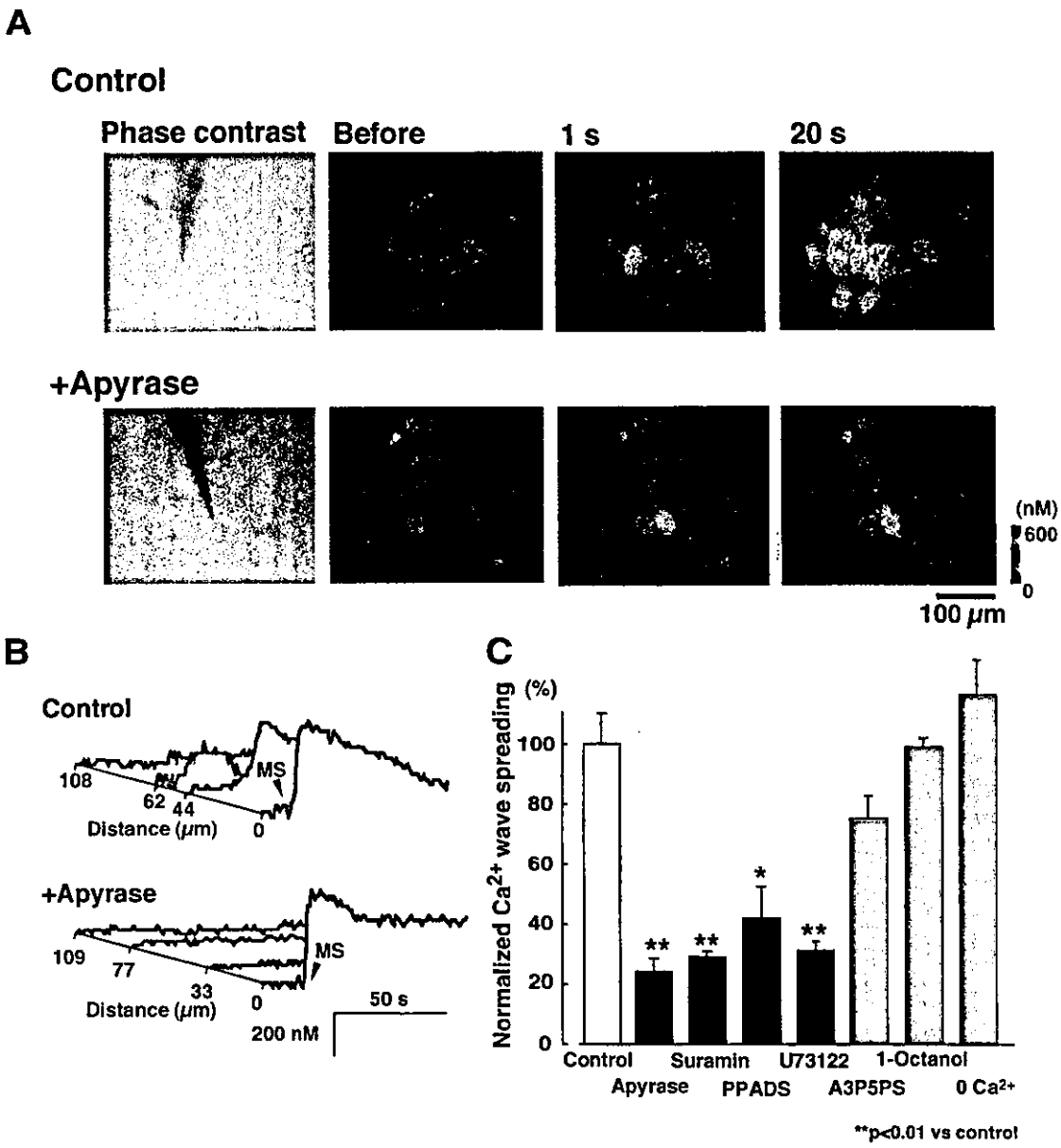

Figure 3 Propagation of Ca^{2+} waves in response to mechanical stimulation in NHEKs

(**A**) Phase-contrast (left) and pseudo $[Ca^{2+}]_i$ images of a field of cultured NHEKs in the absence (upper panels) and presence (lower panels) of apyrase (80 units/ml). Increase in $[Ca^{2+}]_i$ was estimated by ratiometric fura 2 fluorescence ($\Delta F_{340}/F_{360}$) and was then converted into absolute $[Ca^{2+}]_i$ using a standard calibration curve. A single NHEK was mechanically stimulated. (**B**) Plots of $[Ca^{2+}]_i$ as a function of time in four individual NHEKs in the microscopic field. The plots for the non-stimulated cells (blue, green and red traces) horizontally regressed in proportion to their distance from the stimulated cell (black traces) as indicated by the scale bar. In a control experiment, mechanical stimulation of NHEK 1 (black trace) resulted in the induction of a Ca^{2+} wave in adjacent cells after a time lag (upper traces). However, in the presence of apyrase (80 units/ml), mechanical stimulation failed to cause increases in $[Ca^{2+}]_i$ in the surrounding NHEKs (lower traces). The diameter of the spreading distance of the Ca^{2+} wave was calculated in the absence and presence of various chemicals and is summarized in (**C**). The average diameter of the Ca^{2+} wave under the control condition was 93.4 ± 9.7 μm ($n = 12$). Suramin (300 μM), pyridoxal phosphate-6-azophenyl-2′,4′-disulphonic acid (PPADS; 100 μM) and U73122 (5 μM) also abolished the propagation of Ca^{2+} waves, but adenosine 3′-phosphate 5′-phosphosulphate (A3P5PS; 100 μM), 1-octanol (500 μM) or removal of extracellular Ca^{2+} (0 Ca^{2+}) failed to inhibit the mechanical-stimulation-evoked Ca^{2+} wave in NHEKs ($n = 8$–12).

DRG neurons was prepared as described in the Experimental section. Figure 5(A) shows an immunohistochemical image of anti-cytokeratin14 (red) and anti-peripherin (green) antibodies, which are markers for the basal layer of keratinocytes and small-sized DRG neurons respectively. When stimulated with 80 mM KCl, almost all peripherin-positive DRG neurons (Figure 5B, green traces) exhibited increases in $[Ca^{2+}]_i$, whereas cytokeratin14-positive NHEKs (Figure 5B, red trace) did not. Both ATP (100 μM) and UTP (100 μM) caused increases in $[Ca^{2+}]_i$ in 71 % of the small-sized DRG neurons (37 out of 52 cells tested; $dF/F_0 = 6.3 \pm 0.8$ for ATP and 5.8 ± 0.6 for UTP; $n = 37$ in four separate experiments), and 73 % of NHEKs (58 out of 79 cells tested; $dF/F_0 = 5.1 \pm 0.7$ for ATP and 4.3 ± 0.4 for UTP; $n = 58$ in four separate experiments). The UTP-evoked increases in $[Ca^{2+}]_i$ in both types of cells were reproducible, and the first and second UTP-evoked responses were almost identical. The average diameter of the small-sized DRG neurons was 21.8 ± 3.5 μm. Suramin (100 μM) inhibited the UTP-evoked increases in $[Ca^{2+}]_i$ in both types of cells (DRG neurons, 10.2 ± 2.1 % of UTP alone, $n = 37$; NHEKs, 32.1 ± 4.6 % of UTP alone, $n = 58$). Thus

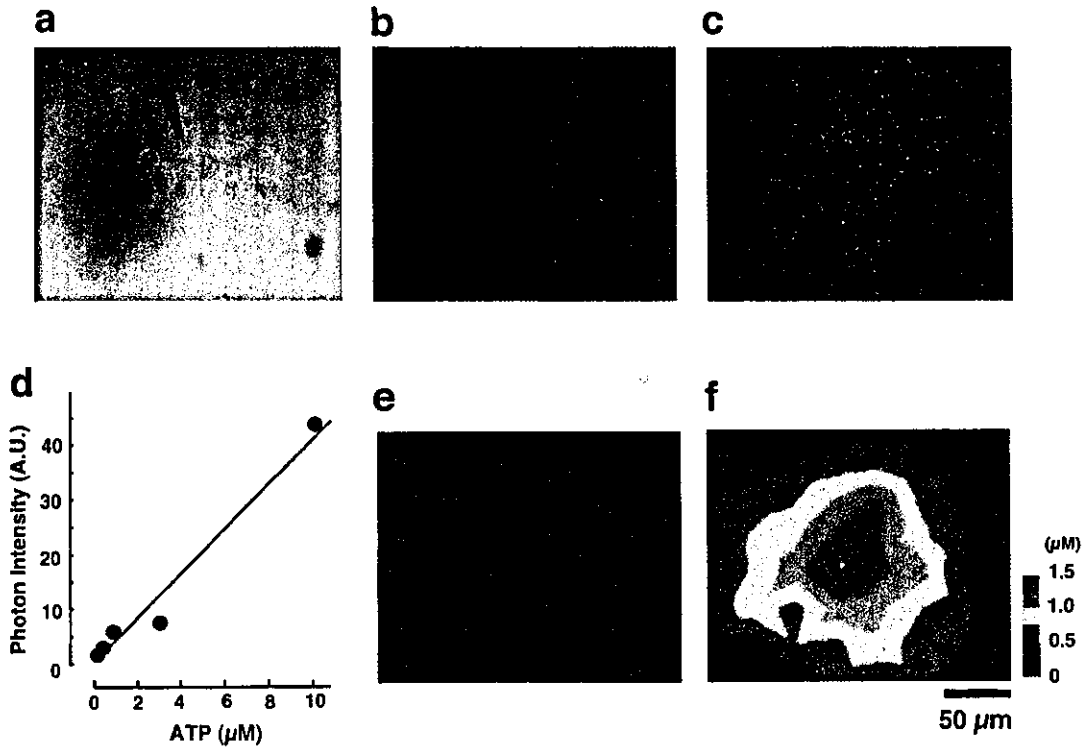

Figure 4 Visualization of release of ATP from NHEKs

The images show photon counts (yellow dots) in a field of NHEKs bathed in luciferin–luciferase reagent before (**b**) and after (**c**) mechanical stimulation. The position of pipette is shown in a phase-contrast image of NHEKs (**a**). (**d**) A typical bioluminescence intensity–ATP concentration relationship under these conditions. Various concentrations of ATP standard solution were injected in the presence of the luciferin–luciferase reagent, and photons were then accumulated for 30 s. (**e**, **f**) Spatial distribution of photon counts of mechanical stimulation shown as a two-dimensional pseudo colour surface plot. Scale bar, 50 μm for images **a**–**c**.

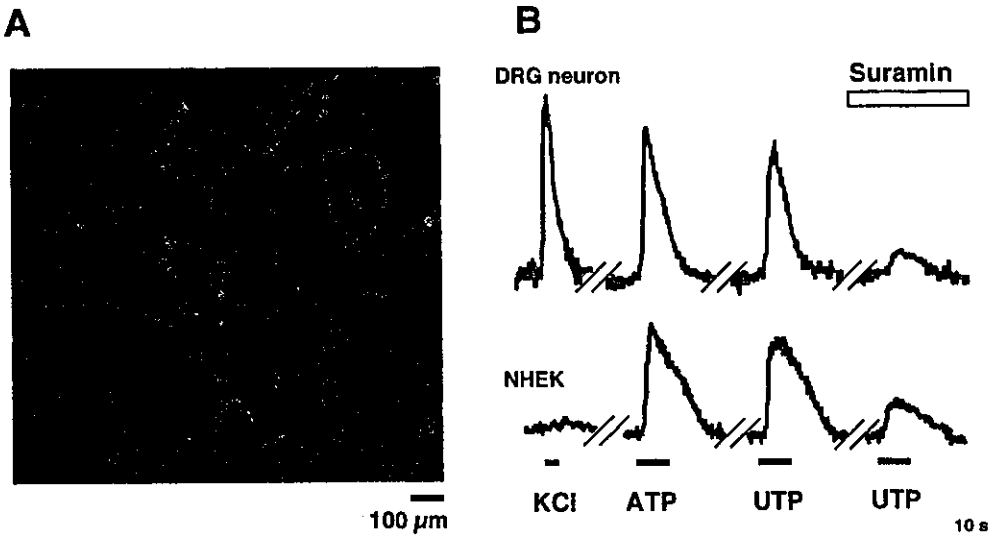

Figure 5 Immunohistochemical staining of DRG neurons and NHEKs

(**A**) After some Ca^{2+} imaging experiments, cells were fixed and stained with anti-cytokeratin14 and anti-peripherin antibodies for confirming NHEKs and small-sized DRG neurons respectively. (**B**) Representative Ca^{2+} responses obtained from self-ratios of fluo-4 fluorescence in anti-peripherin-positive DRG neuron (green) and anti-cytokeratin14-positive NHEK (red). First, cells were stimulated with 80 mM KCl for 3 s. Then, they were stimulated with 100 μM ATP for 10 s and 100 μM UTP for 10 s separated by 5 min. Finally, UTP (100 μM) was applied to the cells in the presence of 100 μM suramin. Both ATP and UTP caused increases in $[Ca^{2+}]_i$ in approx. 71 % of the DRG neurons (37 out of 52 cells tested) and in 73 % of the NHEKs (58 out of 79 cells tested) in the co-cultured cells.

most of the small-sized neurons also expressed UTP-preferring suramin-sensitive P2Y receptors, presumably $P2Y_2$ receptors. In the co-culture of NHEKs and DRG neurons, mechanical stimulation of a single NHEK produced a propagating Ca^{2+} wave in adjacent NHEKs in an extracellular ATP-dependent manner (Figure 6A). Interestingly, this Ca^{2+} wave in the NHEKs was

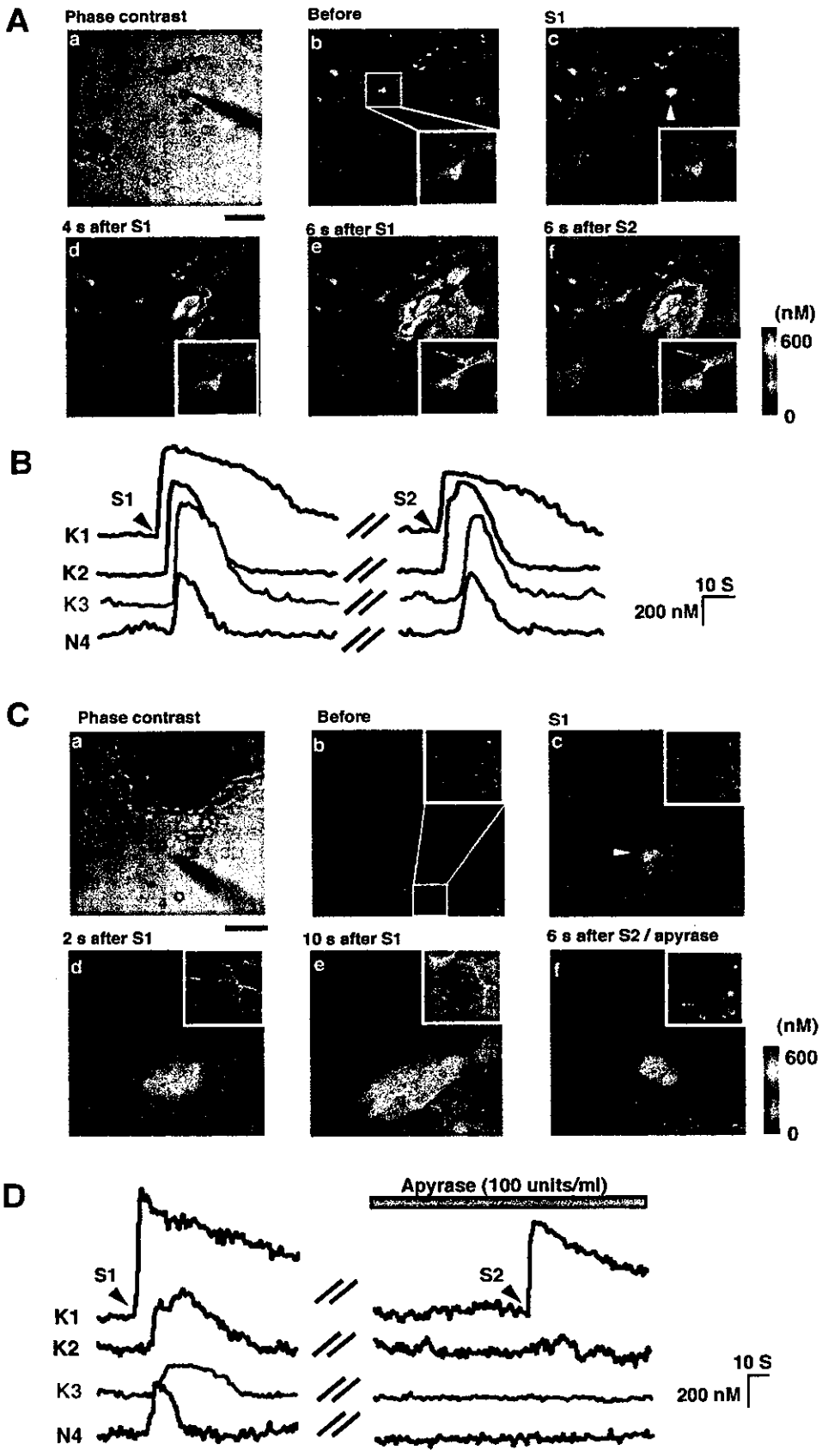

Figure 6 For legend see next page

followed by an increase in $[Ca^{2+}]_i$ in the DRG neurons after a time lag (Figures 6Ae and 6B, trace N4). The increases in $[Ca^{2+}]_i$ in DRG neurons were also dependent on extracellular ATP and the activation of P2 receptors, since the ATP-degrading enzyme, apyrase (grade III, 100 units/ml; Figures 6Cf and 6D), and suramin (100 μM) inhibited the increase in $[Ca^{2+}]_i$ (apyrase, $9.6 \pm 0.9\%$ of S1, $n=21$; suramin, $14.8 \pm 1.9\%$ of S1, $n=33$). Thus we concluded that the release of ATP in response to mechanical stimulation from NHEKs functions as an intercellular molecule between NHEKs and DRG neurons, which may affect nociceptive transduction in peripherin-positive neurons.

DISCUSSION

In the present study, we have demonstrated that ATP is a dominant extracellular signalling molecule in the formation of intercellular Ca^{2+} waves in NHEKs. We also showed that extracellular ATP-dependent Ca^{2+} waves in NHEKs caused increases in $[Ca^{2+}]_i$ in the adjacent DRG neurons. Thus ATP derived from NHEKs functions in both an autocrine and paracrine manner in the peripheral skin-to-sensory neuron system.

Both ATP and UTP caused increases in $[Ca^{2+}]_i$ in NHEKs to a similar extent. These Ca^{2+} responses were independent of extracellular Ca^{2+}, but dependent on inositol 1,4,5-trisphosphate-sensitive Ca^{2+} stores, suggesting the involvement of metabotropic P2Y receptors in the responses. ATP and UTP are natural ligands at $P2Y_2$ receptors, and are approximately equipotent. UTP also activates $P2Y_4$ receptors, but the human $P2Y_4$ receptor is highly selective for UTP than ATP [25]. UDP, an agonist to $P2Y_6$ receptors, only slightly increased the $[Ca^{2+}]_i$ in NHEKs [26,27]. Suramin moderately antagonizes human $P2Y_2$ receptors but not human $P2Y_4$ receptors [28]. NHEKs expressed a large amount of mRNAs for $P2Y_2$ receptors, but not for $P2Y_4$ or $P2Y_6$ receptors. All these pharmacological profiles showed that these responses should be mediated by $P2Y_2$ receptors (Figure 2). Very recently, Greig et al. [29] have reported that skin cells express P2X5, P2X7, $P2Y_1$ and $P2Y_2$ receptors, each of which is expressed in a spatially distinct zone of the epidermis and has distinct cellular functions. $P2Y_2$ receptors are expressed in the lower layer of the epidermis and are involved in proliferation, suggesting that the NHEKs used in the present study might mimic the basal cellular layer of skin cells *in vivo*.

The question remains as to whether endogenous ATP may produce propagating Ca^{2+} waves in NHEKs. Several reports have shown that mechanical stimulation produces a propagating Ca^{2+} wave in non-excitable cells such as astrocytes [15,30] and hepatocytes [12]. In astrocytes, extracellular molecules such as glutamate [11,31] and ATP [15,30], rather than gap junctions [32], are responsible for the propagation of Ca^{2+} waves. We sought to determine whether extracellular ATP produces intercellular Ca^{2+} waves in NHEKs. Mechanical stimulation of a single NHEK resulted in the induction of an intercellular Ca^{2+} wave, which was inhibited by the ATP-degrading enzyme, apyrase, and the P2 receptor antagonist, suramin (Figure 3). The gap junction inhibitor, 1-octanol, had little effect on the Ca^{2+} wave. Imaging of the ATP release by the modified luciferin–luciferase chemiluminescence clearly showed that the levels of extracellular ATP after mechanical stimulation were highest at the site of stimulation and decreased concentrically. These results strongly suggest that the mechanically evoked Ca^{2+} waves in NHEKs are mediated by extracellular ATP and by the activation of $P2Y_2$ receptors. As in astrocytes [15,30], extracellular ATP appears to play a pivotal role in creating the dynamic changes for long-range signalling in NHEKs.

The responses mediated by $P2Y_2$ receptors are probably layer-specific. The ATP-evoked hyperpolarization is very high in the basal layer but extremely low in the suprabasal layer in HaCaT keratinocytes [33]. The mRNA level of $P2Y_2$ receptors is down-regulated in differentiating HaCaT cells [34]. Thus the intercellular Ca^{2+} waves seen in the present study may be a response restricted to the basal layer of keratinocytes *in situ*. The finding that the barrier recovery rate of the mouse epidermis is regulated by functional P2 × 3 [35] suggests that the skin expresses multiple P2 receptors that are linked to distinct physiological functions.

There is an increasing body of evidence that ATP, the predominant extracellular signalling molecule of astrocytes [15,30], may also mediate signalling between neurons and glial cells [36–38]. With regard to the skin-to-sensory neuron system, a similar relationship may also be obtained. Especially, non-myelinated small-sized DRG neurons (nociceptors) terminate in the periphery as free nerve endings [39]. Thus nociceptors can directly contact skin-derived extracellular molecules when skin cells are injured, inflamed or otherwise stimulated. When cells are injured or destroyed, very high concentrations of intracellular ATP (> 5 mM) could leak and affect the surrounding NHEKs and DRG neurons. In the present study, however, we showed that the intercellular Ca^{2+} waves in NHEKs were reproducible when the same cell was stimulated repeatedly (Figure 6). Moreover, the increases in neuronal $[Ca^{2+}]_i$ in response to mechanical stimulation of NHEKs were also reproducible. Thus it appears that extracellular ATP-mediated NHEK-to-DRG neuron communication takes place even when cell damage is not involved. Somatic sensation requires the conversion of physical stimuli into depolarization of the distal nerve endings. It has been reported that activation of $P2Y_1$ receptors in sensory fibres increases the frequency of spikes evoked by a light touch of the skin [40]. Therefore the skin might sense and transmit non-harmful stimuli to sensory neurons via ATP.

DRG neurons express various types of P2 receptors. Ionotropic P2X receptors, especially P2X3 [41] and P2X2 [42] receptors in small- and middle-sized DRG neurons respectively, have been extensively studied in relation to pain. However, recent reports suggest that some P2Y receptors are present in small-sized DRG neurons and are involved in pain signalling. In small-sized neurons, activation of $P2Y_1$ or $P2Y_2$ receptors sensitizes TRPV1 receptors via protein kinase C-dependent mechanisms [43], stimulation of $P2Y_2$ receptors enhances the $[Ca^{2+}]$ increase, leading to the release of CGRP [44], and activation of $P2Y_2$

Figure 6 Dynamic communication between NHEKs and DRG neurons mediated by extracellular ATP

(**A**) Phase-contrast image (**a**) and pseudo colour $[Ca^{2+}]_i$ images (self-ratios of fluo-4 fluorescence; **b–f**) in co-cultured NHEKs and DRG neurons obtained by confocal laser microscopy. The white rectangle field in the middle of image **b** is shown enlarged in the bottom right of images **b–f**. The red arrowhead in image **b** depicts position 4 (DRG neuron 4). The white arrowhead in image **c** shows the initiation of Ca^{2+} wave in response to mechanical stimulation (cell 1). Scale bar, 50 μm. (**B**) The graph shows individual traces of the self-ratios of fluo-4 fluorescence in keratinocytes (K1–K3) and DRG neuron (N4) shown in image **Aa**. Keratinocyte 1 was mechanically stimulated twice (arrows S1 and S2) separated by 5 min. (**C**) Phase-contrast image (**a**) and pseudo colour $[Ca^{2+}]_i$ images (self-ratios of fluo-4 fluorescence; **b–f**) in co-cultured NHEKs and DRG neurons. The white rectangle field in the middle of image **b** is shown enlarged in the top right of images **b–f**. The red arrowhead in image **b** depicts position 4 (DRG neuron 4). The white arrowhead in image **c** shows the initiation of Ca^{2+} wave in response to mechanical stimulation (cell 1). Scale bar, 50 μm. (**D**) The graph shows individual traces of self-ratios of fluo-4 fluorescence in keratinocytes (K1–K3) and DRG neuron (N4) shown in image **a** in **C**. Keratinocyte 1 was mechanically stimulated twice (arrows S1 and S2) separated by 5 min. The first and second mechanical stimulations were performed in the absence and presence of 100 units/ml apyrase (grey horizontal bar).